AD-A035 459 NAVAL SURFACE WEAPONS CENTER WHITE OAK LAB SILVER SP--ETC F/G 1/3
RESPONSE OF A-6 LANDING GEAR DOOR TO AIR SHOCK LOADING.(U)
OCT 76 J G CONNOR

UNCLASSIFIED NSWC/WOL/TR-76-94 NL

| OF |
AD
A035459

END

DATE
FILMED
3-77

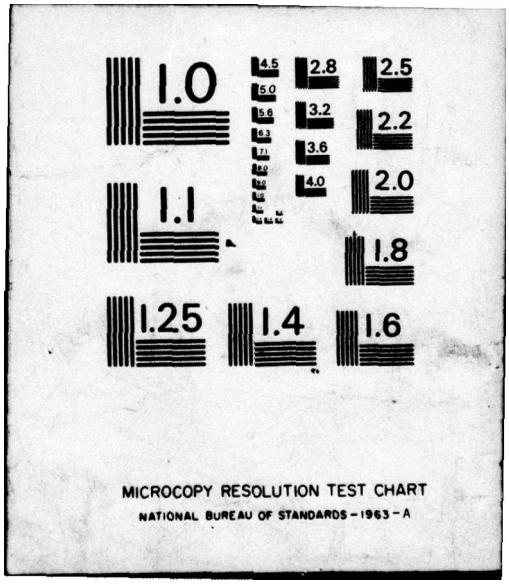
1.0
1.1
1.25
1.4
1.6
1.8
2.0
2.2
2.5
2.8
3.2
3.6
4.0
4.5
5.0
5.6
MICROCOPY RESOLUTION TEST CHART
NATIONAL BUREAU OF STANDARDS - 1963 - A

NSWC/WOL/TR 76-94

NSWC/WOL/TR 76-94

NSWC TECHNICAL REPORT

WHITE OAK LABORATORY

RESPONSE OF A-6 LANDING GEAR DOOR TO AIR SHOCK LOADING

BY
Joseph G. Connor, Jr.

24 OCTOBER 1976

NAVAL SURFACE WEAPONS CENTER
WHITE OAK LABORATORY
SILVER SPRING, MARYLAND 20910

- Approved for public release; distribution unlimited

NAVAL SURFACE WEAPONS CENTER
WHITE OAK, SILVER SPRING, MARYLAND 20910

UNCLASSIFIED

SECURITY CLASSIFICATION OF THIS PAGE *(When Data Entered)*

REPORT DOCUMENTATION PAGE

READ INSTRUCTIONS BEFORE COMPLETING FORM

(14) 1. REPORT NUMBER: NSWC/WOL/TR-76-94

2. GOVT ACCESSION NO.

3. RECIPIENT'S CATALOG NUMBER

(6) 4. TITLE *(and Subtitle)*: Response of A-6 Landing Gear Door to Air Shock Loading.

5. TYPE OF REPORT & PERIOD COVERED: Final TR 10/75 - 4/76

6. PERFORMING ORG. REPORT NUMBER

(10) 7. AUTHOR(s): Joseph G. Connor, Jr.

8. CONTRACT OR GRANT NUMBER(s)

9. PERFORMING ORGANIZATION NAME AND ADDRESS
Naval Surface Weapons Center
White Oak Laboratory
White Oak, Silver Spring, Maryland 20910

10. PROGRAM ELEMENT, PROJECT, TASK AREA & WORK UNIT NUMBERS
63714N; WSL-54;
7W0594-001; 0;

11. CONTROLLING OFFICE NAME AND ADDRESS

(12) 56p.

(11) 12. REPORT DATE: 24 Oct [redacted] 76

13. NUMBER OF PAGES: 53

14. MONITORING AGENCY NAME & ADDRESS *(if different from Controlling Office)*

15. SECURITY CLASS. *(of this report)*: Unclassified

15a. DECLASSIFICATION/DOWNGRADING SCHEDULE

16. DISTRIBUTION STATEMENT *(of this Report)*
Approved for public release; distribution unlimited

(9) Final technical rept. Oct 75-Apr 76,

17. DISTRIBUTION STATEMENT *(of the abstract entered in Block 20, if different from Report)*

18. SUPPLEMENTARY NOTES

19. KEY WORDS *(Continue on reverse side if necessary and identify by block number)*

Shock Loading
Landing Gear Door
Elastic Analysis
Structural Response
NASTRAN
Overpressure
Aircraft Vulnerability

20. ABSTRACT *(Continue on reverse side if necessary and identify by block number)*

Response of an A-6 Aft Main Landing Gear Door to static and transient pressure loads has been calculated with the NASTRAN finite element structural analysis computer code. On the basis of manufacturers static tests these doors have been considered to be the structural items on the plane most sensitive to shock loading. Displacements calculated for static loading compare favorably with those measured on tests. However, examination of the stress distribution in the door panels indicates that the 2.5 psi shock

DD FORM 1 JAN 73 1473 EDITION OF 1 NOV 65 IS OBSOLETE
S/N 0102-LF-014-6601

UNCLASSIFIED

SECURITY CLASSIFICATION OF THIS PAGE *(When Data Entered)*

391 596

limit established by the manufacturer is conservative. The linear elastic NASTRAN stress calculations indicate that at an altitude of 50,000 ft the door should be able to withstand a 3 psi free-field shock normally incident on its outside surface if the peak stress is not to exceed the yield strength. At sea level, the door should withstand a free-field shock of 4.3 psi, normally incident.

NSWC/WOL/TR 76-94 24 October 1976

RESPONSE OF A-6 LANDING GEAR DOORS TO AIR SHOCK LOADING

This report describes an analytical study of the effect of shock loading on the most sensitive item on a critical element list compiled by the plane's manufacturer. Linear elastic calculations were made with NASTRAN (NASA STRuctural ANalysis program). The objective of the study was to determine the greatest amplitude of a peak shock normally incident on the outer skin of the door which would cause the stress in some portion of the door to exceed the yield point of the material.

The work was a part of Advanced Development Objective W48-16X, Nuclear Warfare Survivability of Aircraft.

J. W. Enig

J. W. ENIG
By direction

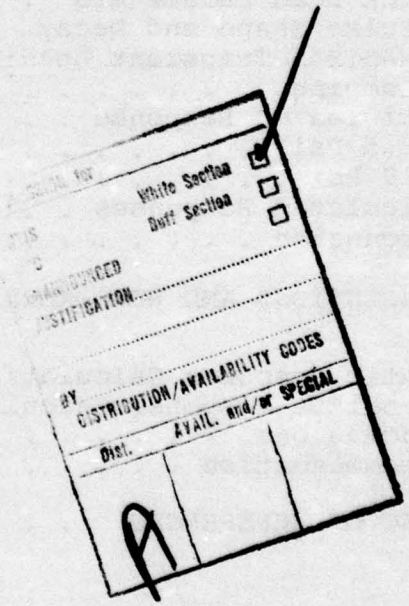

TABLE OF CONTENTS

TABLE OF CONTENTS

TABLES

FIGURES

INTRODUCTION

The Grumman A-6A Intruder is a two man carrier-based all weather fighter bomber which has been in service since the mid 1960's. In combat it may be subject to structural damage from the separate and combined effects of thermal, shock overpressure, and gust loading weapon effects.

Static loading tests were performed by Grumman on various portions of the aircraft to establish its conformance to military specifications, but no dynamic overpressure tests were performed prior to release of the plane to the fleet. In recent years it has become necessary to develop information on the response of various portions of the plane to weapon effect loading, so an analytical study has been undertaken. This effort should be supplemented by experimental testing to establish confidence in the conclusions drawn from the analytical effort.

The present study is a structural analysis of one portion of the A-6 using a large general purpose structural analysis computer code. Static and shock overpressure loads were applied to a finite element model and displacements and stresses were calculated. The calculated static displacements were compared to those determined experimentally during the pre-acceptance testing. The allowable overpressure determined from these static tests is discussed in light of the results of the calculations.

The analytic investigation involved a single structural element - the aft main landing gear door, located on the fuselage under each wing root. This door was chosen because it heads a list of nine critical elements selected on the basis of the pre-acceptance static tests as those most sensitive to overpressure loading (1). These elements are considered critical in the sense that damage to any of them is likely to seriously interfere with aircraft maneuverability or mission completion.

(1). Grumman Aircraft Engineering Corp., "Special Weapons Effects Structural Analysis," Report No. 4121, 15 Feb 1963.

Aft Main Landing Gear Door

Each landing gear door consists of two doubly curved skins and a variety of stiffeners as shown in Figure 1. One door is located under each wing between fuselage stations 228 and 297. In the closed position each door is attached to the fuselage at four points: two hinges at the upper edge, a linkage point in the middle of the aft hinge rib, and a rollor support at the lower forward corner. The doors are made of 7075-T6 aluminum alloy.

Thirteen ribs connecting the two skins lie in planes perpendicular to the axis of the aircraft. Two longerons run along the top and bottom edges of the inner skin and are connected to the outer skin along their entire length. Two other longerons frame a large opening in the inner skin near the forward edge of the door.

The door is designed to sustain an average outward pressure load of 8.62 psi along the upper outward edge and 11.25 psi along the lower inboard edge (2). For limit calculations which led to the allowable overpressure, these loads were represented by a uniform outward pressure load of 10 psi assumed to be applied to the outside skin of the door.

Allowable Overpressures

The allowable overpressure loads on the critical elements were calculated as a part of the pre-acceptance stress analysis. The value for the landing gear door, 2.5 psi, was determined from the design negative pressure on the outside of the door and the allowable compression stress in two angles shown in Figure 1, running the length of the outer skin, one at the top and one at the bottom edge of the door (1). Because insufficient information is given in the report to determine the rationale of the apparently rough calculation, the allowable overpressure value is subject to varying interpretations. It was apparently determined for a static load at sea level; the response of a structure to a dynamic load (3) was not included. Also, shock amplitude amplification due to reflection and altitude were not considered. Yet, this 2.5 psi limit for allowable overpressure, as well as similarly determined values for other portions of the aircraft structure, has been accepted and used in safe delivery determinations for nuclear weapons.

(2). Grumman Aircraft Engineering Corp., "Plan for Fuselage Group Static Tests," Report No. 4133.01, 28 April 1961.

(3) Hall, A. S., The Mechanics of Solids, John Wiley & Sons, Australasia, 1969; p. 328.

Static Tests

To establish conformance to specifications, the manufacturer conducted a series of static tests on many portions of the A-6 structure-including the landing gear door -- before the plane was accepted for service use. Static loads were applied to the door to simulate the critical loading condition: inverted flight at sea level at Mach 0.96 with the doors closed. The loads were applied by a large hydraulic system through bell cranks, walking beams and tension pads with whiffletrees. Incremental loads were measured with a hydraulic pressure gage (2).

Deflections were measured by piano wires attached to the specimen and terminated at graph paper indicators mounted on a vertical board. Dial gages were used sparingly; deflections at several locations exceeded the range of the available gages. No strain measurements were reported, though some strain gages were in place during the tests (2).

For the tests, a structurally complete door was mounted in a fuselage section as it would be found on a plane in service. The fuselage was supported with its plane of symmetry perpendicular to the horizontal test platform with the fuselage reference line parallel to and 100" above it. The fuselage was secured to the test platform with steel jigs; relieving loads were applied as required. Several portions of the door structure were found to yield or buckle during the preliminary tests. These pieces were redesigned and reworked as the tests progressed.

Measurements from these tests (4,5) are included on a graph later in this report, as are results of the calculations which are described in the following sections of this report.

2. FINITE ELEMENT CALCULATIONS

NASTRAN is a large general purpose elastic structural analysis computer code which evolved under the direction of NASA over a period of several years (6). The constant strain finite elements in its library are suited for the analysis of aerodynamic structures (7). Besides determining the effects of static and transient loads on a structure model, the code can perform buckling and vibration eigenvalue analyses on the same model.

(4) Grumman Aircraft Engineering Corp.,"Results of Removable Sections Static Tests," Report No. 4133.31, 22 March 1962.
(5) Grumman Aircraft Engineering Corp., "Results of Removable Sections Static Tests," Report No. 4133.31B. 19 May 1969.
(6) National Aeronautics & Space Administration, "NASTRAN a Summary of the Functions and Capabilities of the NASA Structural Analysis Computer System," Report No. NASA SP-260.
(7) McCormick, C. W., Ed. "The NASTRAN User's Manual (Level 15)," National Aeronautics & Space Admin. NASA SP-222(01), June 1972.

Constructing the finite element model is as much a part of the overall problem as interpreting the results of the calculations. Each grid point of the model must be located in space, and the appropriate elements, with proper material and elastic properties, must be connected among them. Some of the steps involved are outlined in the following paragraphs.

Finite Element Model

The skins, stiffeners and all of the ribs in the door (see Figure 1), were all modeled with NASTRAN's general triangular plate element. This element resists bending, twisting and stretching but does not resist rotation about axes normal to its plane at its corner points.

There are two hat section stiffeners on the inner skin (Figure 1) which resist stresses caused by bending the entire door. These were modeled with the NASTRAN rod element, which resists only torsion and axial tension and compression.

Early in the manufacturers static testing of the door, a longeron was attached to the top edge of the inside surface of the outer skin. This piece was added because of a tendency of the upper edge of the door to buckle near the center of its length. The additional longeron consists of an L section whose sides meet at an angle of about 30°. It was modeled with bar elements, which resist bending as well as extension and torsion.

The two hinge ribs are heavier than the other eleven; these, and the hinges themselves, were also modeled with bar elements.

Skin Geometry

Grid points were placed at the intersections of the ribs and each skin. An additional line of points was placed in each skin midway between neighboring ribs. This allows large areas of the skins to be represented by nearly equilateral triangles approximately 2" on a side. Grid point coordinates were specified in a rectangular system coincident with aircraft coordinates as shown in Figure 2. The origin is 100 inches below the axis of symmetry of the fuselage in a plane perpendicular to this axis and passing through the nose tip. The Z axis is parallel to the axis of symmetry, +Y, is outward from the fuselage, and +X is upward. These axes are referred to, respectively, as the fuselage station, buttock line, and water line coordinates on the drawings from which the measurements were taken.

Since no drawings were available from which accurate coordinates could be determined for grid points located between ribs on the doubly curved skin surfaces, a smoothing procedure was devised as follows. Coordinates of the midplane of each skin along each rib

were read from scale drawings of the ribs (8). Two quadratic surfaces, separately least-square fitted to the points for each skin, allow coordinates of points anywhere on either skin to be determined by substitution. This procedure also smooths out the irregularities necessarily introduced by reading values from scale drawings. Approximately 45 points were used to determine the quadratic for each skin. The resulting equations of the two surfaces are:

Outer skin (elliptic paraboloid):

$$Y = 30.84 + \tfrac{1}{2}(-3.921\ X^2 + 772.5\ X - 37663 + 10.39\ Z)^{\frac{1}{2}}$$

Inner skin (hyperbolic paraboloid):

$$Y = 38.95 + \tfrac{1}{2}(2.145\ X^2 - 270.8\ X + 7342 + 3.333\ Z)^{\frac{1}{2}}$$

Points determined from these expressions represent the intersections of the skins with planes normal to the symmetry axis of the plane. The ribs are taken to lie in these planes. To use the expressions, one specifies a fuselage station (Z) and several water line (X) values corresponding to skin/stiffener intersections; a buttock line value (Y) is then calculated from the expressions for each ZX combination. At each fuselage station either 5 or 6 points were specified on the inner skin and 7 on the outer skin. A total of 295 points were chosen to cover both skins. An additional point near the upper end of each hinge rib allowed the hinges to be connected to the fuselage.

Deck Preparation

Since the large number of geometry and connection cards are similar among themselves, hand punching is highly susceptible to error. This is particularly true because there are several hundred of each type of card. Errors are sometimes obvious and easily corrected, but are often rather subtle and not immediately evident. Thus, the geometry and plate connection cards were punched by FORTRAN preprocessing programs written specifically for the purpose. NASTRAN does not include such routines primarily because each problem is unique and too much computer memory space would be required to cover a sufficient number of cases.

The first step in preparing the NASTRAN deck was to find suitable equations for the geometrical surfaces from which coordinates of arbitrary points on the two skins could be determined. The results of the least square fitting technique were discussed in the preceding section of this report. The equations so determined were used by a second program which calculated coordinate values and assigned

(8) Grumman Aircraft Engineering Corp., Drawings,: "Frame Installation:" 128B11201, 128B11328, 128B11329, 128B11330, 128B11331, 128B11332
"Intercostal Installation:" 128B11337

sequence numbers to grid points in the model. A third program assigned these grid point numbers in proper sequence to the corners of all the triangular flat plates elements in the model.

The fewer bar and rod element connection cards were punched by hand. Also prepared by hand were the cards which specified the material properties of the elements and those which describe the various loads which were applied.

The grid coordinate and element connection cards were fed into a plotting program to check the model for glaring mistakes or inconsistencies. This program, IDEAL, was written at the Navy NASTRAN office the DTNSRDC, Carderock. Perspective views and any desired cross sectional cuts can be displayed on a CRT and can be obtained in hard copy to facilitate corrections between runs. Several views of the final model are shown in Figures 3 through 6.

The last preliminary step was the generation of a set of grid resequencing cards. A code, BANDIT, also written at NSRDC, punches cards to be included in the NASTRAN deck which optimize the grid point numbering sequence. The renumbering is done to minimize the semi-bandwidth of the element stiffness matrix used in the NASTRAN calculations. This resequencing is internal to NASTRAN, i.e., it has no effect on requests for output, which must be made in terms of the original numbering scheme. The only effect is a significant reduction in computer running time required for the problem.

3. FAILURE CRITERIA

Structural failure occurs when a structure has been loaded to such an extent that it has been rendered incapable of performing its required function. Structures generally fail by rupture, collapse or excessive distortion. Like the skin of any aircraft, the A-6 landing gear door can suffer some skin buckling without detrimental effect. Distortion to such an extent that the door cannot be closed will cause an increase in aerodynamic drag forces, perhaps large enough that the plane becomes difficult to manuver. Large distortion may be accompanied by yield failure of portions of the skin and ribs, further increasing drag.

This report will determine a threshold load -- the greatest peak shock overpressure at which yield failure does not occur.

Buckling

Critical buckling stresses are compressive and usually well below the elastic limit of the material of the structure. However, if an element in compression happens to be appropriately restrained, elastic buckling is less likely than for an unconfined element. Stresses then may increase with load until the elastic limit is exceeded, culminating in local or general collapse of the structure.

In tension there is no tendency to buckle. Element stresses increase to balance loads, and excessive stretching occurs when stresses exceed the yield strength of the material.

Column Buckling. Buckling of the bar and rod elements in the A-6 landing gear door model would be expected at axial compressive load levels equal to or greater than the Euler critical load. However, for the loading conditions on the door and the locations of the bars and rods in the model, it appears likely that all of them are in tension or light compression. This intuition is borne out by examination of stress output. Thus, Euler column buckling is not anticipated.

Plate Buckling. Critical buckling stresses for plates in biaxial compression depend on edge restraints. For square plate buckling the algebraic sum of two orthogonal edge stresses is given by (9):

$$\sigma_1 + \sigma_2 = \frac{10.693}{a^2}\left[\frac{.823\ E\ t^2}{1-\nu^2}\right] \qquad \text{(Clamped, 4 edges)}$$

$$\sigma_1 + \sigma_2 = 2\left[\frac{.823\ E\ t^2}{1-\nu^2}\right] \qquad \text{(Simply Supported)}$$

A typical plate element in the A-6 door model has the following properties:

$E = 10.3 \times 10^6$ psi = elastic modulus
$t = 0.050$ in = plate thickness
$a = 2.5$ in = edge length
$\nu = 0.33$ = Poisson's ratio

$$\left[\frac{.823\ E\ t^2}{1-\nu^2}\right] = 23778$$

Buckling of such a plate might then be anticipated at the following stress levels:

$\sigma_1 + \sigma_2 = 40{,}681$ psi (clamped edges)

$\sigma_1 + \sigma_2 = 47{,}555$ psi (simply supported edges)

Equivalent Stress Theory

The octahedral shear stress theory of failure gives the same results as the energy of distortion method (10). These are the two theories most used in flight vehicle structural design.

(9) Roark, R.J., Formulas for Stress and Strain, McGraw-Hill Book Company, New York, 1965.
(10) Bruhn, E. F., Analysis and Design of Flight Vehicle Structures, Tri-State Offset Company, Cincinnati, Ohio, 1965.

According to the octahedral shear stress theory, inelastic action at any point in a body under combined stress action begins only when the octahedral shear stress becomes equal to $\frac{\sqrt{2}}{3}\ \sigma_{ty} = 0.47\ \sigma_{ty}$, where σ_{ty} is the tensile yield strength determined from a standard tensile test. Tensile and compressive yield strengths are assumed to be the same.

The octahedral shear stress can be expressed in terms of the three principal stresses:

$$\tau_{oct} = (1/3)\ [(\sigma_1 - \sigma_2)^2 + (\sigma_2 - \sigma_3)^2 + (\sigma_3 - \sigma_1)^2]^{\frac{1}{2}}$$

Define an equivalent stress:

$$\overline{\sigma} = (\tau_{oct})/(0.47) = \left(\frac{3}{\sqrt{2}}\right) \tau_{oct}$$

For a biaxial stress state ($\sigma_3 = 0$), this reduces to:

$$\overline{\sigma} = + [\sigma_1^2 + \sigma_2^2 - \sigma_1\sigma_2]^{\frac{1}{2}}$$

If $\overline{\sigma} \geq \sigma_{ty}$ for the given material, then inelastic action occurs.

Failure

Local buckling will occur in a structure wherever the algebraic sum of two orthogonal principal stresses exceeds about 40,000 psi. However, buckling displacements should not occur rapidly enough to relieve the initial high stresses produced by a blast load. If an elastic solution produces an equivalent stress exceeding the yield strength of an element, then yield failure is more likely than buckling.

In the following analysis, emphasis will be on finding skin elements in which equivalent stresses approach or exceed yield. As mentioned above, aircraft skins are designed to accommodate a certain amount of elastic buckling, so yield failure is considered the more important phenomenon.

4. STATIC ANALYSIS

Static elastic displacements were calculated with NASTRAN to compare with the measured displacements described earlier. Below is an outline of the calculations, a comparison of calculated and measured displacements, and a discussion of the stress field in various portions of the door.

Static pressure loads are applied to the NASTRAN model by indicating a pressure value and requiring NASTRAN to determine the equivalent forces on grid points. All NASTRAN calculations are performed in terms of grid point displacements; other quantities are related to the displacements through the properties of the finite elements which connect the points.

However, it should be noted that calculated displacements are not directly comparable to the measured displacements observed during the static tests since the four support points in the NASTRAN model are not free to move relative to the equilibrium position of the fuselage. During the static tests, the door was mounted on a fuselage which could, and did, undergo deformation and rigid body translation when loads were applied. A correction was applied to the calculated displacements before comparing them with measurements.

Load Subcases

One outward and four inward directed pressure loads were applied to the calculational model. The inward pressures were 2.5, 5.0, 10.0, and 20.0 psi; the outward pressure was 10.0 psi. All were applied normal to the plane of each plate element on the outer skin of the model.

Results of the five cases were what should be expected for a perfectly elastic system. The values of stress and displacement for each of the inward load conditions were in the same ratio as the loads; that is, the displacements and stresses output for the 10 psi load were four times those for the 2.5 psi load, double those for the 5 psi load, and half those for the 20 psi load. Also, when the direction of the load was reversed (from 10 psi inward to 10 psi outward) the output quantities changed in sign but not in magnitude. As indicated, these observations were expected, since NASTRAN assumes perfect elasticity regardless of load level or direction.

10 Psi Load

On the landing gear door, the design ultimate load* arises from internal pressurization and flight induced aerodynamic loads. It is an outward pressure varying from 11.25 psi along the upper edge to 8.62 psi along the lower edge of the door (2). This distribution was averaged by Grumman (1) to be equivalent to a uniform 10 psi outward applied to the outer skin of the door.

As noted above, NASTRAN-calculated responses to inward and outward directed pressure loads differed in sign but not magnitude. Since our ultimate interest here is inward directed load response, the following discussion is based on NASTRAN calculations for 10 psi inward directed loads.

* Design ultimate load is defined as 1.5 times the largest flight load anticipated during normal operation of the aircraft.

Displacements. During the static tests, normal displacements were measured at eight points on the outer skin of the door. Exact locations of these points are not specified; they are described only as near the corners, near the center of each edge (except the bottom edge), and near the center of the door. Also, as mentioned above, the fuselage on which the door was mounted was free to suffer distortions and rigid body translations. The test loads were applied with an intricate hydraulic device which pulled on a limited number of pressure pads fastened to the outer skin; that is to say, the loads were not applied uniformly to the entire surface of the door.

The three points mentioned in the preceding paragraph make direct comparison between the measurements and the NASTRAN calculations somewhat tenuous. NASTRAN calculated the displacements of precisely located points and the support points in the model are not free to move. Also, a uniformly applied load was used in NASTRAN which differs from the discretely applied static loads used in the static tests.

NASTRAN computes three mutually orthogonal components of displacement at each grid point. In the aircraft coordinate system, no one of these components is normal to the outer surface of the door. The three components must be combined vectorially to find the component normal to the door, a quantity similar to that measured on the static tests. The vector addition was done with a small code written for the purpose.

Static test data has been taken from the Grumman report of the tests (4). Normal displacements at three points, roughly along the center line of the door are shown in Figure 7 for three design loads: limit*, yield**, and ultimate. A correction eliminated some of the effect of the fuselage displacement as the load was applied: each measured displacement was reduced by an effective fuselage displacement, which could not be the same for each point because the fuselage stretches out of shape as well as translating with the applied load. The displacement of the middle of the forward edge of the door was reduced by the average of the fuselage displacements near the top and bottom edge of the door. The center displacement was reduced by the average of the fuselage displacements at the lower forward and upper aft edges. Finally, the average fuselage displacement at the upper and lower aft edge was subtracted from the displacement of the center of the aft edge of the door. These corrections are somewhat arbitrary, though they appear reasonable in view of the minimal information available.

Comparison of the measured points with the NASTRAN-calculated curve shows that, at least from the point of view of the resulting displacements, the uniformly applied 10 psi inward load is most

* Design Limit Load is defined as the largest anticipated operational load.
** Design Yield Load is defined as 1.15 times the limit load.

nearly equivalent to the design yield load. This conclusion is somewhat nebulous because of the impossibility of making direct point-by-point comparisons, the rigidity of the support points in the NASTRAN model, and the difference in the manner of load application.

Structure Deformations. Several computer-drawn sketches have been included to show the effect of the 10 psi inward load on the model. In all of them, the displacements due to the load are exaggerated by a factor of about 10. The sketches show only a line joining grid points which are connected by elements in the model; no details of the structural element are illustrated.

Figure 8 shows the deformed and undeformed shapes of the longeron which was added to the upper edge of the door. This member was modeled with end-to-end BAR elements. The grid points shown in this sketch are actually connected by three elements between each neighboring pair: the two BARs which form the angled longeron, and one edge of the flat plate TRIA2 element in the outer skin. Only a single line is shown. There are no major changes in curvature which would imply buckling or local yielding. Thus, the redesigned longeron functions as intended.

The ribs and stiffeners which support the inner and outer skins are shown in Figure 9. The perspective view is from a vantage point just aft and outside the door on the port side of the plane. The forward end is thus foreshortened, while the aft end, closer to the viewer, is somewhat enlarged. Again, no sharp curvature changes are observed, so no major buckling of the door is expected with a 10 psi static load.

Stress Distribution. For this model, with a 10 psi inboard-directed static load, the greatest equivalent stress was found to be 40,319 psi in plate element 378 on the inner skin. Stresses in most of the plate elements are less than 25,000 psi. The yield strength of the aluminum alloy from which the door was fabricated is about 70,000 psi (11). This and other properties of the alloy are listed in Table I.

As mentioned earlier, buckling at the center portion of the upper (hinge) edge of the door required the addition of a stiffening longeron. Also, during static testing, the upper end of the rib at fuselage station 258.5 parted on several tests. (This station is just forward of the center of the door.) The rib was strengthened so that it withstood the static ultimate load test without failure (4).

(11) MIL-HDBK-5B: "Metallic Materials and Elements for Aerospace Vehicle Structures," 1 September 1971.

The largest stresses in the model under this load were found in the vicinity of the center of the door's length near the strengthened rib. Outer skin stresses are compressive; the largest equivalent stress noted was 39,763 psi (element 118). Also, the longerons which join the inner and outer skins along the entire length of the door exhibit stresses in the 30,000's. Inner skin stresses are tensile; in one element (378) the equivalent stress reached 40,319 psi. In the hat sections, edge stiffeners, and hinge ribs(-- the elements represented by bars and rods in the model --- the axial stresses are not large enough to be of concern, seldom exceeding 10,000 psi.

It appears that failure, if it occurs, will be in a mode which involves crimping or parting of one of the two longerons at the top and bottom edges, severe buckling of the outer skin, or yield failure of the inner skin. Failure is most likely near the center of the door in the neighborhood of the strengthened rib.

In Figures 10 through 13 areas of the model in which stresses exceed 18,500 psi are indicated. This value was chosen for ease of comparison with the transient load analysis which will be discussed later in this report. The relatively few elements in which stresses exceed 30,000 psi are also indicated; these elements are the ones most likely to fail in the case of an extreme loading condition.

No stresses were measured during the static testing, thus no comparison of the NASTRAN output with those experiments can be made. Stress calculations are presented (12),but the regions of the door for which the calculations were made are not identified sufficiently to permit a meaningful comparison.

5. TRANSIENT ANALYSIS

In the Grumman weapons effects analysis (1) the design limit load was used to determine an allowable overpressure load of 2.5 psi for the landing gear door. It does not appear that the dynamic response characteristics of the structure or the effects of altitude on a shock were accounted for in the derivation.

One can estimate the dynamic response of a structure to a long duration incident shock wave of peak amplitude P as follows. At relatively low pressures at sea level and for nearly normal incidence, one can assume that the reflected peak pressure will be double the incident, or 2 P. In addition, the long duration reflected load can be approximated by a sudden increase, or step function, in pressure. Now, peak displacements and stresses in an elastic system subjected to a step function load are approximately double those for a static

(12) Grumman Aircraft Engineering Corp., "Fuselage Stress Analysis, Part II, Fuselage Mid-Section," Report No. 4108.21, 22 Mar 1963.

load of the same amplitude. Thus, a shock loaded elastic system may experience stresses and displacements four times as great as those determined for a static load equal in amplitude to the incident shock overpressure.

According to this reasoning, a normally incident 2.5 psi peak overpressure shock (at sea level) would be expected to produce maximum displacements and stresses in the landing gear door equivalent to those produced by a 10 psi static load. Thus, one can infer that the 2.5 psi limit in the A-6 literature was based on a line of reasoning similar to that outlined above. However, strict interpretation of the Grumman analysis (1) does not support this conclusion because it is implied in the analysis that the 2.5 psi limit is an allowable overpressure acting as a uniform static load. Previous vulnerability analyses have also treated the 2.5 psi limit as a static overpressure load capacity (13).

In the 10 psi NASTRAN static load analysis, it was found that the greatest equivalent stress was 40,319 psi. Since the yield strength of the skin material is about 70,000 psi, it would appear that the door could take a static load of 10(70,000/40,319) = 17.4 psi without failure.

Shock Load Parameters

A 1 Kt explosion was assumed as the source for the shock loads in this problem. The source and target were taken to be at the same altitude: 50,000 ft. Computer costs per load case for NASTRAN transient analyses are five to seven times greater than for static runs, so it is not economical to run a range of load cases and later choose the one or ones most appropriate to the problem at hand.

Two cases were considered sufficient to bracket response of the landing gear door: a 2.5 psi shock front acting side-on and a 5 psi shock front normally reflected (at 50,000 ft altitude). The important consideration to the NASTRAN calculation is the actual pressure load applied to the plane, not whether it is derived from an incident or a reflected shock front, at sea level or altitude.

A limit load of 2.5 psi is given in the A-6 literature, and treated as a side-on pressure, it was taken as the lower bound for the calculations. Since the static calculations indicated that the door could withstand a 17.4 psi load without yield failure, a 2.5 psi side-on transient load, even with the dynamic amplification factor of 2, should not induce yield failure.

(13) Classified Reference.

The choice of the upper bound was also based on the static result that the door can withstand a 17.4 psi load. In Table II it is seen that at an altitude of 50,000 ft a 5 psi shock front produces a reflected peak shock overpressure amplitude of about 19 psi. Yield failure would be expected from this load because the static 17.4 psi load will produce yield stresses in the door; the dynamic amplification factor will ensure that peak stresses exceed yield strength.

The peak amplitude of reflected shocks at altitude was determined from the tabulations in reference (14). For comparison, shock parameters for several yields and two incident overpressures are listed in Table II at sea level and at 50,000 ft. Note that the ratio of reflected to incident shock overpressure increases with altitude for a given incident overpressure; this is due to the fact that the reflected pressure depends on shock strength (the ratio of shock overpressure to ambient pressure) rather than shock overpressure alone.

Positive phase durations were determined from tabular listings in reference (15), and are included in Table II.

Pulse Shape and Decay. Immediately behind a shock front, pressure decays steeply, then tapers off and slowly approaches zero at the end of the positive phase. There is no generally applicable decay law which applies to all such decays at all pressure levels from all sources.

However, the modified Friedlander decay law reproduces pressure gage signatures almost exactly at 7.5 psi shock overpressure, and can be used with reasonable accuracy from 0 to 25 psi (15). An expression of this law is (16):

$$P = P_o(1 + t/t_+)\ e^{-b(t/t_+)}$$

Where:

P = overpressure at time t, at some point (psi)

P_o = initial peak overpressure (psi)

t = time after shock arrival at the point (sec)

t_+ = positive duration (sec)

b = decay constant

An expression for the decay constant is:

$$b = 0.365\ (P_o)^{\frac{1}{2}}$$

(14) Swisdak, M. M., Jr., "Explosion Effects and Properties Part I - Explosion Effects in Air," NSWC/WOL/TR 75-116, 6 October 1975.

(15) Classified Reference.

(16) U.S. Army Materiel Command, "Explosions in Air, Part I," AMC Pamphlet AMCP 706-181, 15 July 1974.

This is based on HE data (17); upon comparison, it was found to reproduce nuclear data in reference (15) quite closely. It was therefore used in the present problem. For 2.5 psi, b is found to be 0.58; for 19 psi it is 1.59.

Although positive phase durations for an incident shock and the reflected pulse produced by it are somewhat different, they have been assumed equal for purposes of this study. Durations were determined from graphical data presented in reference (15). For 2.5 psi, t_+ is approximately 400 msec, and for 5 psi, t_+ is nearly 300 msec.

Combining all of the above information, the following Friedlander expressions were used to specifiy the time varying loads applied to the NASTRAN model of the landing gear door:

$P = 2.5\ (1 + t/.4)\ e^{-1.45\ t}$ for 2.5 psi peak pressure;

$P = 19\ (1 + t/.3)\ e^{-5.3\ t}$ for 19 psi peak pressure.

NASTRAN Transient Loading. The NASTRAN Normal Mode module can be used to determine the mechanical resonances of a model structure. Several calculations were made for the landing gear door covering different frequency intervals. The lowest normal mode frequency found was 89.2 hz. The longest natural period is therefore 11.2 msec and the quarter period is 2.80 msec.

Choice of rise time for the load applied to a NASTRAN model is dictated by the following considerations. As far as the structure is concerned, a load must have a rise time less than about one tenth the time to the first maximum in the response (0.28 msec in the present case) in order to appear to the structure as an impulsive load. However, zero rise time should not necessarily be used to represent a shock load in a NASTRAN problem because of the way the program treats a step load: the load applied to the model is the mean value of the maximum and minimum values at the step. Thus, the load an a structure would be an unrealistic two step jump if a zero rise time were used. The rise time of the loads applied to the NASTRAN model of the door was arbitrarily chosen to be 0.1 msec; it is not zero and it is much less than one tenth the quarter period of the structural resonance.

The duration of the loads of interest are several hundred milliseconds (see above) or many times the natural period, but response during only the first 20 msec following application of the load was calculated. This allows time for one complete cycle of the natural vibration in addition to permitting startup instabilities to settle out. Later time behavior has no effect on responses calculated in

(17) Potter, R., and Jarvis, C. V., "An Experimental Study of the Shock Wave in Free Air from Spherical Charges of TNT and 60/40 RDX/TNT," United Kingdom Atomic Energy Authority, AWRE 01-73.

the first 20 msec. Output was requested at only 1 msec intervals; this minimized required computer running times and still permitted accurate determination of peak response, the most important parameter. The 19 psi transient load used for this problem is shown in Figure 14.

Transient loads must be applied to a NASTRAN model in terms of three time-independent orthogonal force components at each grid point. There is no provision, similar to that available for static calculations, for internally transforming normal pressure on flat plate elements into force components at grid points. In addition, static loads as such cannot be included in a transient calculation; such loads can only be included as constant amplitude transient loads of long duration, or as equivalent distortions of the elements. No loads of this kind were applied in the transient problem runs; i.e., the door structure is not prestressed. It is assumed part of a plane in level flight at a constant speed.

For a transient analysis, more information must therefore be added to the NASTRAN data deck beyond the items required for static analyses. Three orthogonal force components must be specified for each grid point. The component of a given load in each direction is some fraction of the load; the fraction is the component of 1.0 psi load in the given direction. Another card in the deck then provides a factor to change the effective pressure load to the desired value (for a 10 psi load the factor is 10; for a 5 psi load, it is 5; and so on). Still other cards provide information to NASTRAN about the time dependence of the load.

Rather than preparing all these cards by hand, the force components on all grid points from a NASTRAN run for a 1.0 psi static load were obtained as punched output. These were converted to the proper format for transient analyses, and an interpolation table was included which lists pressure values at various times according to the shape and duration values discussed earlier.

Damping. When a structure is struck an impulsive blow it settles into vibration at its fundamental frequency. That the vibration eventually ceases implies the existence of damping forces - which may be supplied by special damping coatings, by friction at the many riveted, welded or hinged joints in the structure, or by intermolecular friction in the material of which the structure is made. A measure of the amount of damping is the loss factor, which is not amenable to precise measurement since its value depends as much on the construction of a structure as on the material used in the fabrication.

Loss factor is the fractional amount of kinetic energy dissipated in each cycle of vibration. It is also twice the fraction of

critical damping present in the structure. A value for the loss factor, or damping ratio, typical of aircraft structures is 10^{-2} (18).

The equation of motion for a one dimensional damped harmonic oscillator can be written as follows:

$$M\ddot{X} + b\dot{X} + kX = F$$

(where the symbols have their usual meanings)

Assuming sinusoidal displacements at frequency ω, this equation can be written:

$$-\omega^2 M X + b\, i\omega\, X + k X = F$$

or $$-\omega^2 M X + k(1 + i\, g) X = F$$

$$g = \text{loss factor} = \omega(b/k)$$

Damping, treated this way is referred to as complex stiffness (for the obvious reason) or uniform structural damping -- a term more appropriate to the present discussion. In the transient analysis of the A-6 door performed with NASTRAN, this type of damping is supplied uniformly to every finite element in the model Both the loss factor and the frequency at which it dominates (the fundamental resonance of the structure) must be specified.

As a separate problem, NASTRAN calculated the normal mode frequencies and mode shapes of a structure within a specified frequency range. If the range is restricted properly, the fundamental frequency of the structure can be determined; for the A-6 door, the lowest normal mode frequency was found to be 89.2 hz.

So, for the transient analyses, the following parameter values were used:

$$g = 0.01$$

$$\omega = 89.2 \text{ hz} = 560.5 \text{ radians/sec}$$

Anticipated Response

Peak transient response can be estimated from the response to a static load. The ratio of the first peak value of a transient displacement or stress response to the same response to a static load is the product of two factors. One factor is the ratio of the load amplitudes: since NASTRAN treats the model as a completely linear elastic structure, responses should be in the same ratio as the loads. This was found to be true for the landing gear door when

(18) Ungar, E. E., "The Status of Engineering Knowledge Concerning the Damping of Built-up Structures," Journal of Sound and Vibration 26(1) 141-54 (1973).

static load responses were compared. The other factor is due to the fact that the response of an elastic structure to an impulsive load is double that observed for a static load of the same amplitude.

2.5 Psi. Peak displacement and stress response to a normally incident 2.5 psi peak free-field overpressure shock should be related to the same responses to a 10 psi hydrostatic load as follows:

$$(2.5 \text{ psi Transient Response}) = (10 \text{ psi Static Response})(f_p)(f_t)$$

where: f_p = free-field peak pressure ratio = 2.5/10 = 0.25

f_t = dynamic reflection factor = 2

Thus:

$$TR_{2.5} = 0.5\ SR_{10}$$

19 Psi. Peak responses for this transient load can be determined from the following factors:

$$f_p = 19/10 = 1.9$$

$$f_t = 2$$

and:

$$TR_{19} = 3.8\ SR_{10}$$

The compressive yield stress is about 70,000 psi for the alloy used in the door. Thus regions in which equivalent stress reaches or exceeds 70000/3.8 = 18500 psi for the 10 psi static load are those most likely to fail under the normally reflected 5 psi (or 19 psi) transient load. These regions were highlighted in the previous discussion of the 10 psi static response (Figures 10 through 13).

Calculated Responses

All displacements and stresses calculated for both transient loads ring at about the same frequency: 85 hz. First peaks occur near 6 msec but the exact time of the peaks and precise frequencies cannot be determined from the calculations because of the relatively coarse 1 msec time step. Accelerations, as well as stresses and displacements all peak at approximately 6 msec after application of the load. Velocity peaks occur midway in time between the peaks of the other quantities, as they should since velocity is the derivative of displacement and the integral of acceleration. Assuming harmonic ringing, the vibrations are sinusoidal, and the velocity is 90° out of phase with displacement and acceleration.

Displacement, velocity and acceleration of the grid point (# 149) near the center of the door are shown in Figures 15, 16, and 17.

The values shown are the components normal to the surface of the door at the grid point for both loads. The static displacements shown dotted in Figure 15 were calculated from the 10 psi static response by multiplying it by the ratio of the transient pressure amplitude to 10 psi. We see that the peak displacement is only slightly less than twice the static prediction. Also, the transient oscillations appear to be centered about the static prediction.

The equivalent stress, previously discussed under "Failure Criteria", for element 118 is shown together with the static values for each load in Figure 18. Element 118 is the one which exhibits the largest equivalent stress value in the entire model of the door. For the 19 psi load, the equilibrium or average stress is about 75,000 psi, slightly above the yield point of the door material (~70000 psi). This implies that yield failure is likely to occur in this element at this load level.

Stresses in several elements and displacements of points in the outer skin near the center of the door are listed in Tables III through VII. Ratios corresponding to those discussed in the previous section are included. Elements and points chosen for this tabulation were selected because they experienced the largest responses in the door for every load case.

That the ratios in all cases are lower than anticipated should be expected because the pressure load has decayed from its peak (Figure 14) by the time the response peaks and because of the damping forces introduced for the transient analyses. The ratios are 6 to 7% lower than predicted for the 2.5 psi load, and 8 to 9% low for the 19 psi load. Velocities in the latter case are greater than in the former, so the velocity-dependent damping forces play a larger role in the response behavior. Since the rate at which damping forces do work is greater, the fraction of the energy imparted to the door by the impulsive load dissipated as heat is larger for the 19 psi load.

Discussion

Two transient loads have been applied to a lightly damped structure. The large load was intended to indicate the failure threshold; the smaller was not expected to produce failure - but is the currently accepted value of transient failure load.

The smaller load, 2.5 psi side-on, did not induce failure, here taken to be the production of stress beyond the yield point. The larger load, 5 psi normally reflected, on the other hand, led to failure according to this definition. Both these loads are stated as free-field overpressures at 50,000 ft altitude.

The peak equivalent stress observed when a 19 psi reflected pressure acts on the structure is 140,675 psi (in element 378 on the

inner skin near the lower edge of the door). The maximum permissable stress is assumed to be the yield point, or 70,000 psi. For the linear elastic system the maximum acceptable reflected pressure is therefore 19(70,000/140,675) = 9.4 psi. Interpolation in the tables in reference (14) shows that this reflected pressure would be produced by a 3 psi side-on shock normally incident on the A-6 door at 50,000 ft altitude. Thus, if peak stress is not to exceed yield, a normally reflected 3 psi shock front will be the threshold of failure at 50,000 ft.

The NASTRAN calculations determine the response of the door to a load without regard to altitude, weapon yield or other parameters. At 50,000 ft failure will occur for normally incident shock fronts greater than 3 psi. However, the controlling parameter is the reflected peak overpressure load: 9.4 psi. Figure 19 is a plot of the free field overpressures which produce this reflected pressure at various altitudes (14). It can be seen that, for a given free-field shock overpressure, the liklihood of failure due to a normally reflected shock is less at lower altitudes. The door should withstand loading by a 4.3 psi shock normally reflected from its outer skin at sea level.

In the discussion of the calculations for 10 psi static load it was observed that the maximum equivalent stress determined from the NASTRAN output was 40,319 psi (in element 378 on the inner skin). Since failure is assumed to occur when some stress in the door reaches yield (70,000 psi), this implies that the door can withstand a static load of 10(70,000/40,319) = 17.4 psi. The equivalent short rise time transient load peak should then be half this value, or 8.7 psi (3).

The transient analysis showed that a transient load of 9.4 psi would produce yield. This load is about 8% higher than that determined from the static analysis. Part of the difference is due to the decay of the pressure pulse from its peak of 19 psi to its value at 6 msec (18 psi) -- a drop of about 5% (see Figure 14). The remainder of the difference is due to the effects of damping in the transient analysis. Because of the decaying load and the retarding effects of damping, stresses do not build up immediately and a somewhat higher initial peak amplitude can be tolerated in a transient analysis.

Strict interpretation of the 2.5 psi limit imposed by the manufacturer as the static capability leads to the conclusion that the door can withstand dynamically a reflected pressure pulse of 1.25 psi. A more widespread, and looser interpretation of the 2.5 psi limit will allow the plane to be flown in any region in which the free field overpressure is less than 2.5 psi. From the NASTRAN analysis, it is concluded that the plane can operate safely in any region in which the normally reflected pressure does not exceed 9.4 psi. The significance of these various treatments of structural capability is best shown in Table VIII where the safe ranges are given as a function of altitude for the three methods. It is seen that they can differ by as much as a factor of four.

6. CONCLUSIONS AND RECOMMENDATIONS

Static Response Calculations

An inward directed 10 psi static load was applied normal to the outer skin surface of the finite element model of the landing gear door. Displacements calculated were comparable to those observed experimentally when the design yield load was applied to the actual door (see Figure 7). (The design yield load is defined to be 15% greater than the design limit load, which, in turn, is the greatest expected operational flight load.)

With this 10 psi load, stresses in a few portions of the model approached 40,000 psi -- slightly more than half the yield strength of the material used.

Transient Response Calculations

All transient calculations were based on the assumption of a 1 Kt weapon detonated at a coaltitude of 50,000 ft with the plane, at the stand-off distance appropriate to the desired shock over-pressure.

Two inward shock loads were applied normal to each element of the outer skin of the door model. Based on the static calculations, a 2.5 psi side-on peak amplitude load, the lower of the two cases, was not expected to induce severe damage. However, one interpretation of the manufacturer's 2.5 psi limit leads to the conclusion that it is the maximum permitted shock load on the door. It is based on static measurements, and is the basis for including the landing gear door on the list of critical shock sensitive items on the plane. Peak displacements for this load were less than 0.5" and peak stresses were found to be less than 20,000 psi.

The greater of the two loads, 5 psi normally reflected at 50,000 ft, was expected to induce excessive stresses in the outer skin and some ribs. This expectation was also based on the static calculations. Indeed, peak displacements of the order of 3" and peak stresses approaching 140,000 psi were calculated, indicating yield failure of portions of the door. High stresses were found in the same regions of the door as in the static calculations, and the magnitudes could be roughly predicted from the corresponding static values.

Primary failure will occur in two locations: the central portion of the outer and inner skins; and the longerons which join the outer and inner skins at the top and bottom edges of the door. The outer skin suffers compressive yield with attendant buckling, and the inner skin and longerons fail in tensile yield.

Failure will be initiated by reflected shock overpressures in excess of 9.4 psi striking the door at any altitude. At 50,000 ft altitude, a 3 psi incident free-field overpressure will produce the limiting reflected pressure of 9.4 psi. At sea level, as shown in Figure 19, 9.4 psi reflected is produced by a 4.3 psi incident free-field shock amplitude. This is greater than the 2.5 psi indicated in the manufacturer's list of critical elements (1). Thus, the list, based on static loading tests, tends to be conservative.

Conclusions

The Aft Main Landing Gear Door is probably the most shock sensitive element on the A-6, though not necessarily at the level stated in the manufacturer's test reports. Interpretation of the results of this study indicates that the door should survive a 3 psi free-field shock at 50,000 ft altitude or a 4.3 psi free-field shock at sea level, irrespective of the orientation of the door with respect to the shock front.

Recommendations

Field testing with explosion loads should be conducted on an A-6 aircraft instrumented with strain and displacement gages at points for which calculation results are available. Application of known explosion pressure loads will produce stress and displacement distributions for comparison to those calculated in the present investigation. Comparison with tests should substantiate the conclusions of this study. Specifically, the ambiguities surrounding yield load evaluation should be cleared away.

Simultaneously, the longer duration gust loading effects would be recorded for the plane as a whole. A coarser finite element model of the plane should then be constructed and run on NASTRAN for comparison with these measurements.

LIST OF REFERENCES (in order of citation)

1. Grumman Aircraft Engineering Corp., "Special Weapons Effects Structural Analysis," Report No. 4121, 15 Feb 1963.

2. Grumman Aircraft Engineering Corp., "Plan for Fuselage Group Static Tests," Report No. 4133.01, 28 April 1961

3. Hall, A. S., The Mechanics of Solids, John Wiley & Sons, Australasia, 1969; p. 328

4. Grumman Aircraft Engineering Corp., "Results of Removable Sections Static Tests," Report No. 4133.31, 22 March 1962.

5. Grumman Aircraft Engineering Corp., "Results of Removable Sections Static Tests," Report No. 4133.31B, 19 May 1969.

6. National Aeronautice & Apace Administration, "NASTRAN, A Summary of the Functions and Capabilities of the NASA Structural Analysis Computer System," Report No. NASA SP-260.

7. McCormick, C. W., Ed., "The NASTRAN User's Manual (Level 15)," National Aeronautics & Space Administration, NASA SP-222(01) June 1972.

8. Grumman Aircraft Engineering Corp., Drawings:
"Frame Installation": 128B11201, 128B11328, 128B11329, 128B11330, 128B11331, 128B11332;
"Intercostal Installation," 128B11337

9. Roark, R. J., Formulas for Stress and Strain, McGraw-Hill Book Company, New York, 1965.

10. Bruhn, E. F., Analysis and Design of Flight Vehicle Structures, Tri-State Offset Company, Cincinnati, Ohio, 1965.

11. MIL-HDBK-5B: "Metallic Materials and Elements for Aerospace Vehicle Structures," 1 September 1971.

12. Grumman Aircraft Engineering Corp., "Fuselage Stress Analysis, Part II, Fuselage Mid-Section," Report No. 4108.21, 22 March 1963.

13. Classified Reference.

14. Swisdak, M. M., Jr., "Explosion Effects and Properties Part I - Explosion Effects in Air," NSWC/WOL/TR 75-116, 6 October 1975.

15. Classified Reference.

REFERENCES (Cont.)

16. U.S. Army Materiel Command, "Explosions in Air, Part I," AMC Pamphlet, AMCP 706-181, 15 July 1974.

17. Potter, R., Jarvis, C. V., "An Experimental Study of the Shock Wave in Free Air from Spherical Charges of TNT and 60/40 RDX/TNT," United Kingdom Atomic Energy Authority, AWRE 01-73.

18. Ungar, E. E., "The Status of Engineering Knowledge Concerning the Damping of Built-up Structures," Journal of Sound and Vibration 26(1) 141-54 (1973).

TABLE I. Properties of 7075 T-6 Aluminum (Reference 11)

Elastic Modulus = E =	10×10^6 psi
Shear Modulus = G =	3.9×10^6 psi
Poisson Ratio = ν =	0.33
Density = ω =	0.101 lb/in^3
Yield Point =	70,000 psi (0.050" plates)
=	74,000 psi (< ½" bars, rods)
Ultimate Strength =	77,000 psi (0.050" plates)
=	82,000 psi (< ½" bars, rods)

TABLE II. Shock Wave Data

Altitude (ft)	Yield (Kt)	Side-on Overpressure (psi)	Reflected Overpressure (psi)	Range (ft)	Duration (msec)
50,000	1	2.5	7.64	1192	379
		5	18.97	864	296
	10	2.5	7.64	2568	817
		5	18.97	1861	638
	100	2.5	7.64	5533	1759
		5	18.97	4010	1374
Sea Level	1	2.5	5.36	1900	290
		5	11.39	1210	245
	10	2.5	5.36	4093	624
		5	11.39	2607	528
	100	2.5	5.36	8819	1346
		5	11.39	5616	1137

TABLE III. Stresses in Elements Along Upper Edge of Door

BAR elements are stiffeners in the plane of the skin

the TRIA2 element in each case is the neighboring outer skin element.

Stresses in the BAR elements are axial stresses;
Stresses in the TRIA2 elements are equivalent stresses, defined in the text.

Element	Static Stress 10 psi load (psi)	Peak Transient Stress (at 6 msec) 2.5 psi load (psi)	(ratio)	19 psi load (psi)	(ratio)
BAR 831	22740	10563	.46	79634	3.50
TRIA2 1097	18502	8688	.47	65506	3.54
BAR 832	22663	10600	.47	79916	3.53
TRIA2 1109	18478	8678	.47	65433	3.54
BAR 833	22731	10620	.47	80068	3.52
TRIA2 1121	19963	9199	.46	69354	3.47
Predicted Ratios:			.50		3.80

TABLE IV. Equivalent Stresses in Outer Skin

Center of door, top to bottom.

TRIA2 Element	Static Stress 10 psi load (psi)	Peak Transient Stress (at 6 msec) 2.5 psi load (psi)	(ratio)	19 psi load (psi)	(ratio)
1097	18502	8688	.47	65506	3.54
101	12214	5905	.48	44538	3.65
102	30435	14507	.48	109396	3.59
103	28931	13700	.47	103311	3.57
104	32278	15040	.47	113415	3.51
105	31760	15131	.48	114086	3.59
106	33449	15734	.47	118632	3.55
107	33011	15375	.47	115912	3.51
108	8852	3946	.45	29739	3.36

TABLE V. Equivalent Stresses in Longeron at Lower Edge of Door

(Note: TRIA2 Element 477 Abuts Element 108, Listed in TABLE IV.)

TRIA2 Element	Static Stress 10 psi load (psi)	Peak Transient Stress (at 6 msec) 2.5 psi load (psi)	(ratio)	19 psi load (psi)	(ratio)
477	4014	*		12959	3.23
479	11823	5574	.47	42035	3.56
480	36434	17032	.47	128420	3.52
481	10476	5100	.47	38455	3.67
482	38413	17903	.47	134984	3.51
483	15253	7127	.47	53727	3.52
484	37041	17215	.46	129787	3.50
485	14788	6948	.47	52385	3.54

* not available in output from transient runs

TABLE VI. Equivalent Stresses in Most Highly Stressed Elements

TRIA2 element	Static Stress 10 psi load (psi)	Peak Transient Stress (at 6 msec) 19 psi load (psi)	(ratio)
118 (center of outer skin)	39763	137880	3.47
378 (top edge, center, inner skin)	40319	140675	3.49

TABLE VII. Normal Displacements at Center of Door.

Grid Point (Location)	Static Displ. 10 psi load (in)	Peak Transient Displ. (at 6 msec) 2.5 psi load (in)	(ratio)	19 psi load (in)	(ratio)
141 (top edge)	-0.785	-.379	.48	-2.86	3.64
149 (center)	-.826	-.385	.47	-2.90	3.51
153 (bottom edge)	-.727	-.328	.45	-2.47	3.40

TABLE VIII

Safe Range vs Altitude for Various Interpretations of Door Capability.

Altitude (ft)	Ranges (ft)		
	Method 1	Method 2	Method 3
0	5600	1900	1360
10000	5098	1688	1246
20000	3887	1490	1205
30000	3370	1348	1183
40000	2892	1279	1139
50000	2570	1213	1110

(Yield = 1 Kt)

Method 1: 2.5 psi static capability, 1.25 psi normally reflected pressure at all altitudes

Method 2: 2.5 psi free field overpressure at any altitude.

Method 3: NASTRAN analysis of 9.4 psi normally reflected pressure at all altitudes.

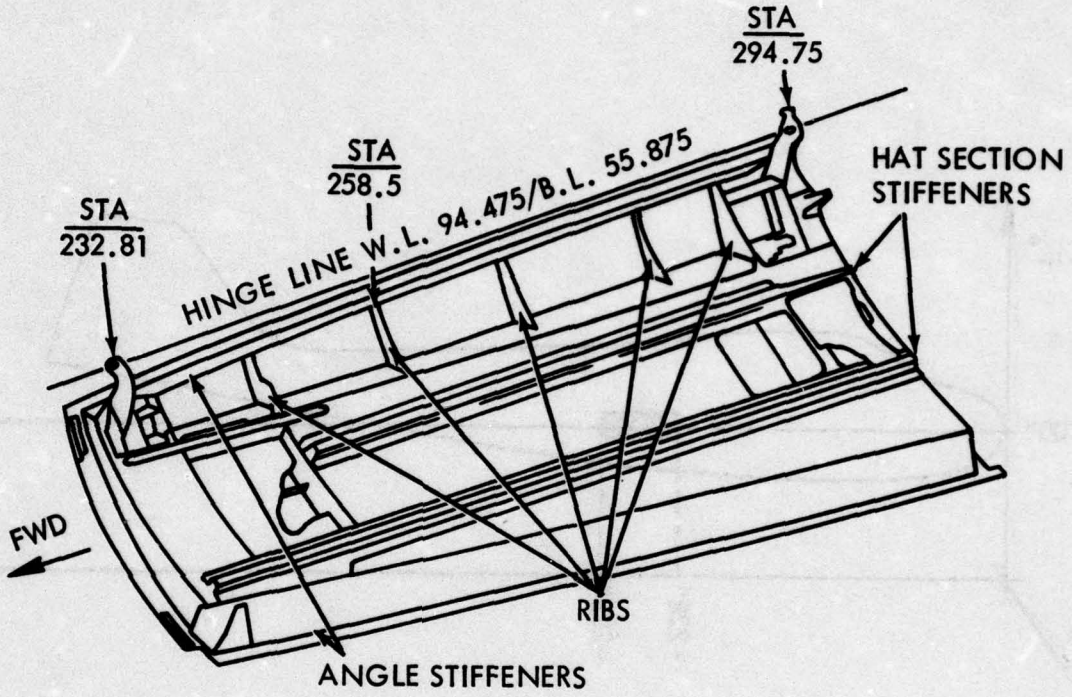

FIG. 1 AFT LANDING GEAR DOOR (STARBOARD SIDE)

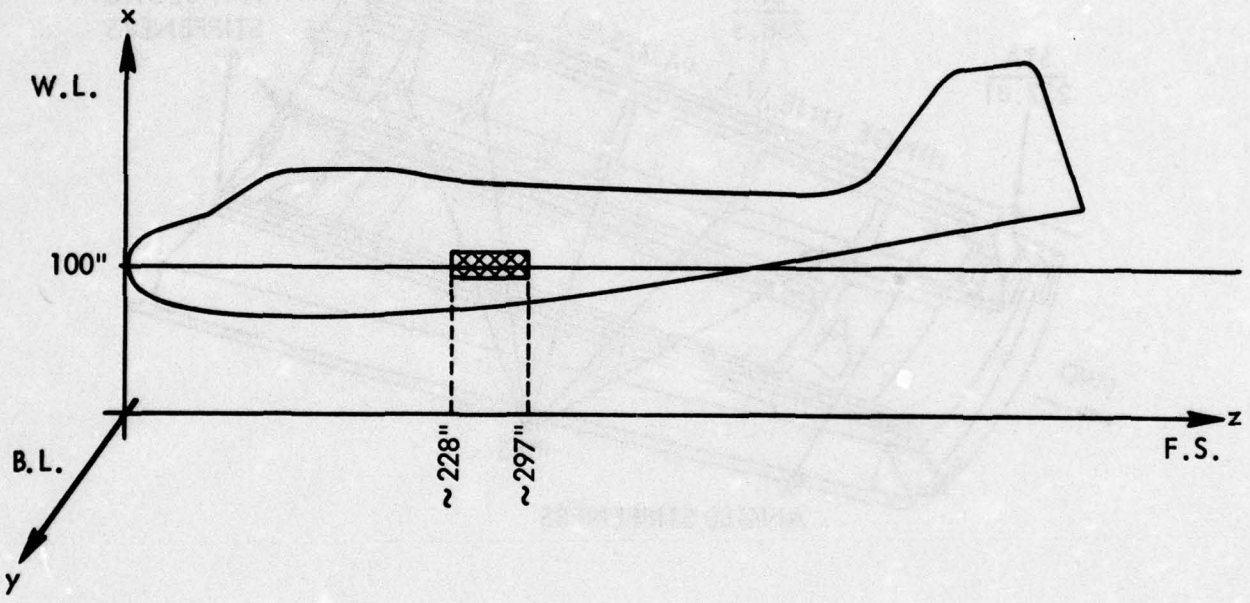

FIG. 2 COORDINATE SYSTEM FOR NASTRAN DATA INPUT

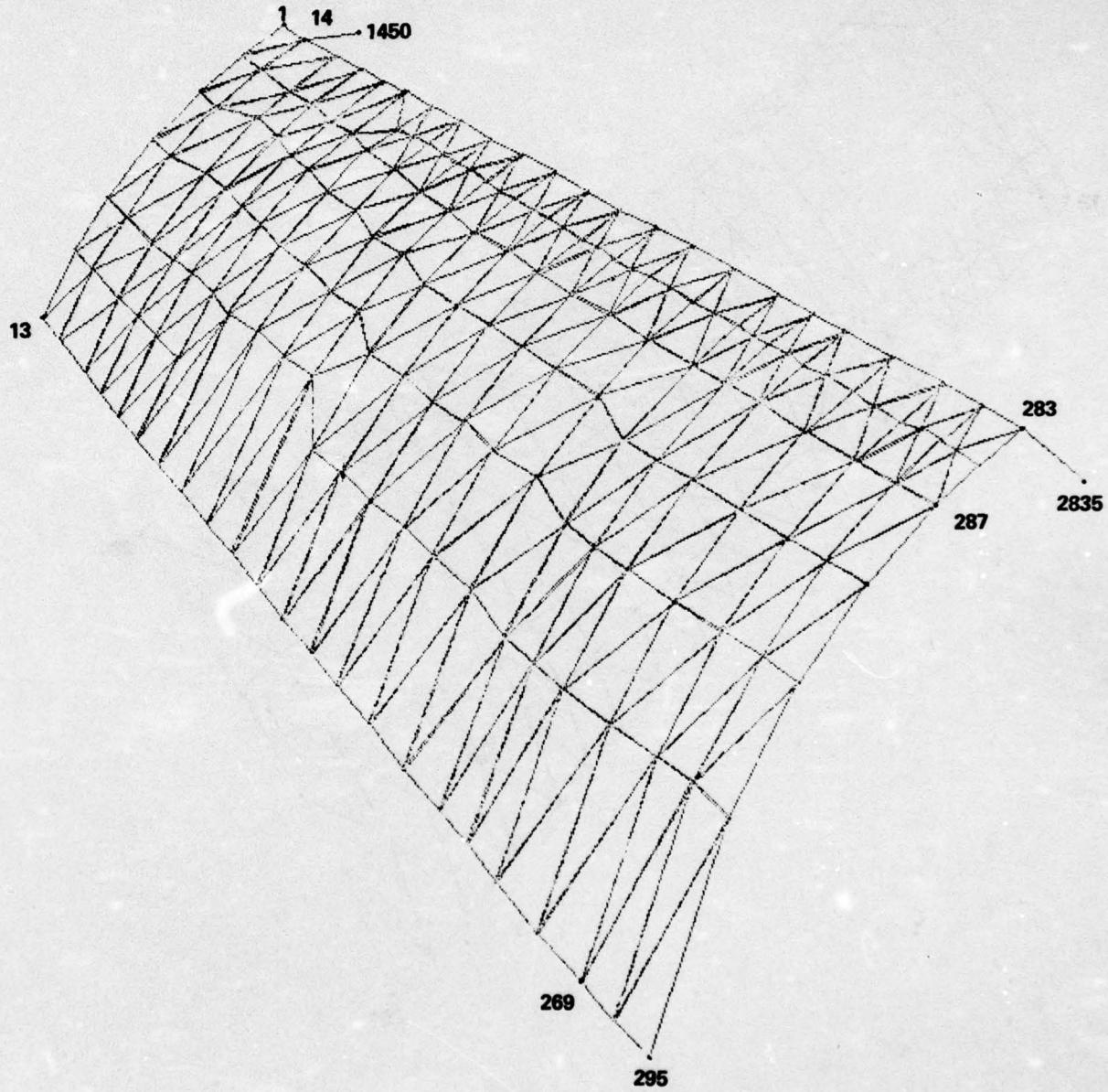

FIG. 3 OUTER SKIN MODEL

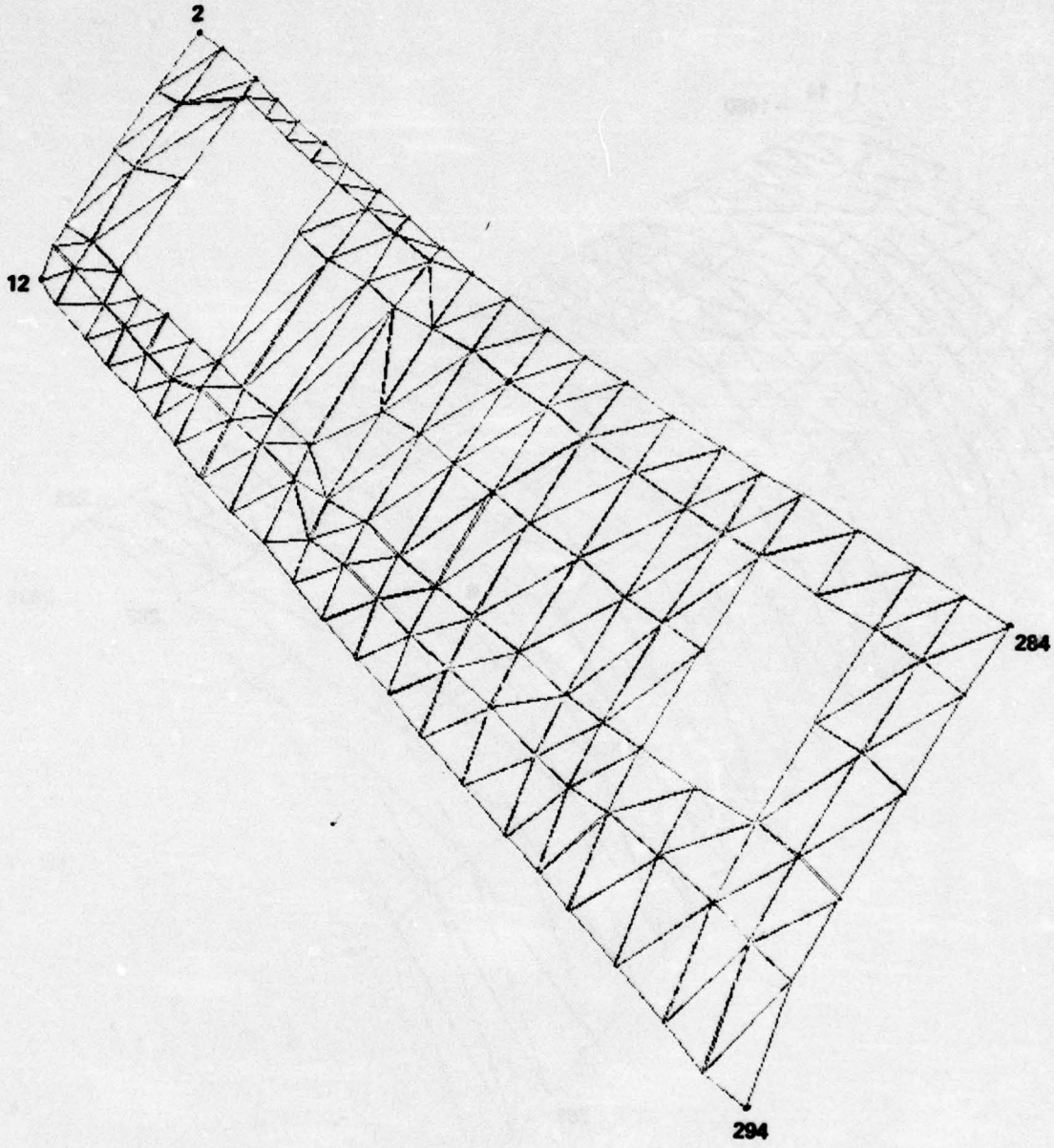

FIG. 4 INNER SKIN MODEL

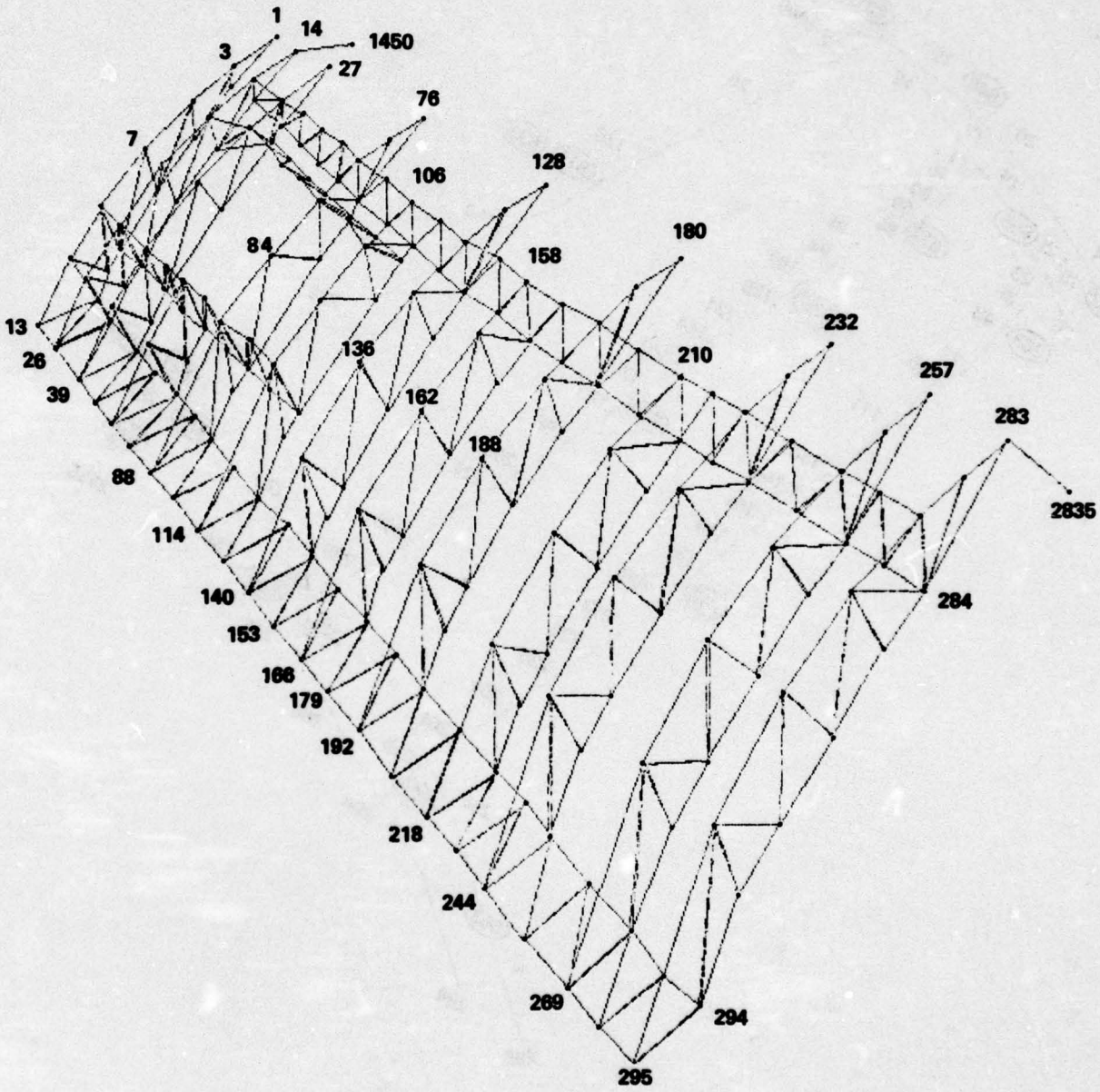

FIG. 5 RIB AND LONGERON PORTION OF MODEL

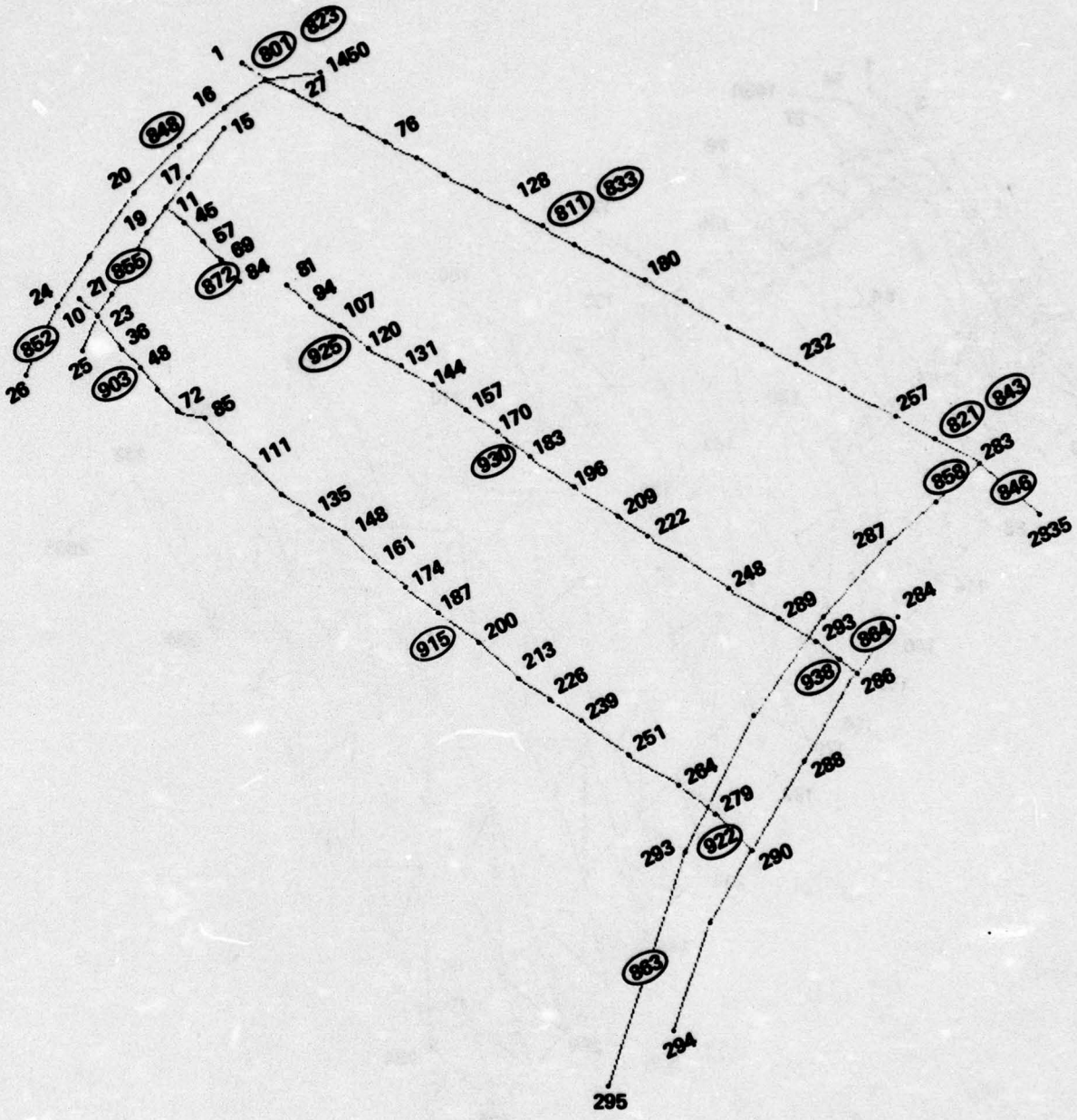

FIG. 6 BAR AND ROD STIFFENERS

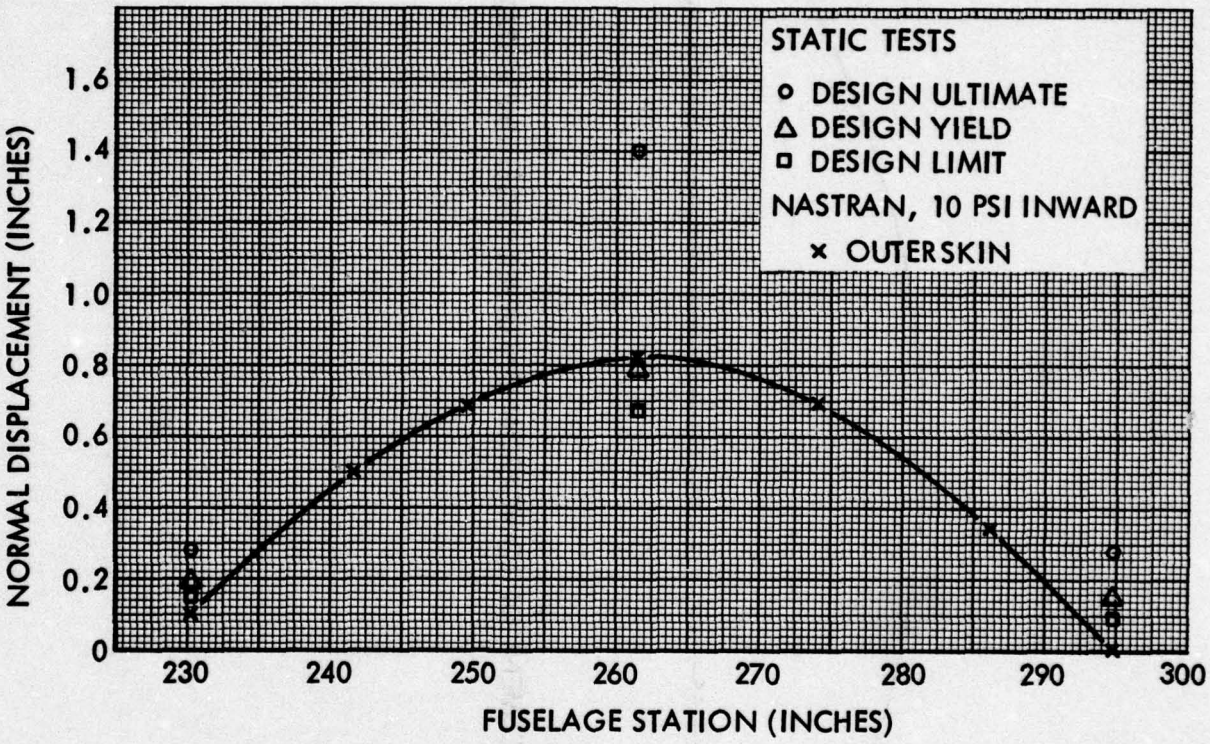

FIG. 7 NORMAL DISPLACEMENT OF OUTER SKIN ALONG CENTER LINE OF DOOR

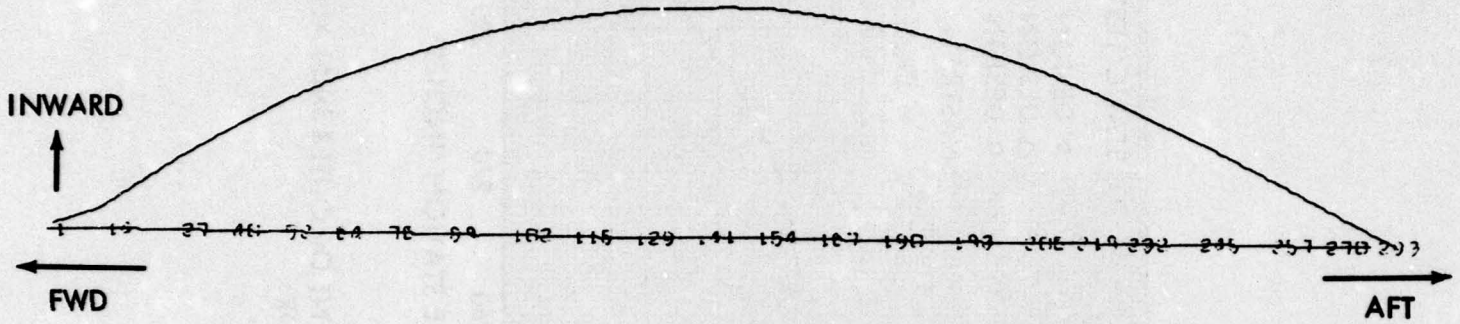

FIG. 8 DISPLACEMENT OF LONGERON ON UPPER EDGE; 10 PSI STATIC LOAD

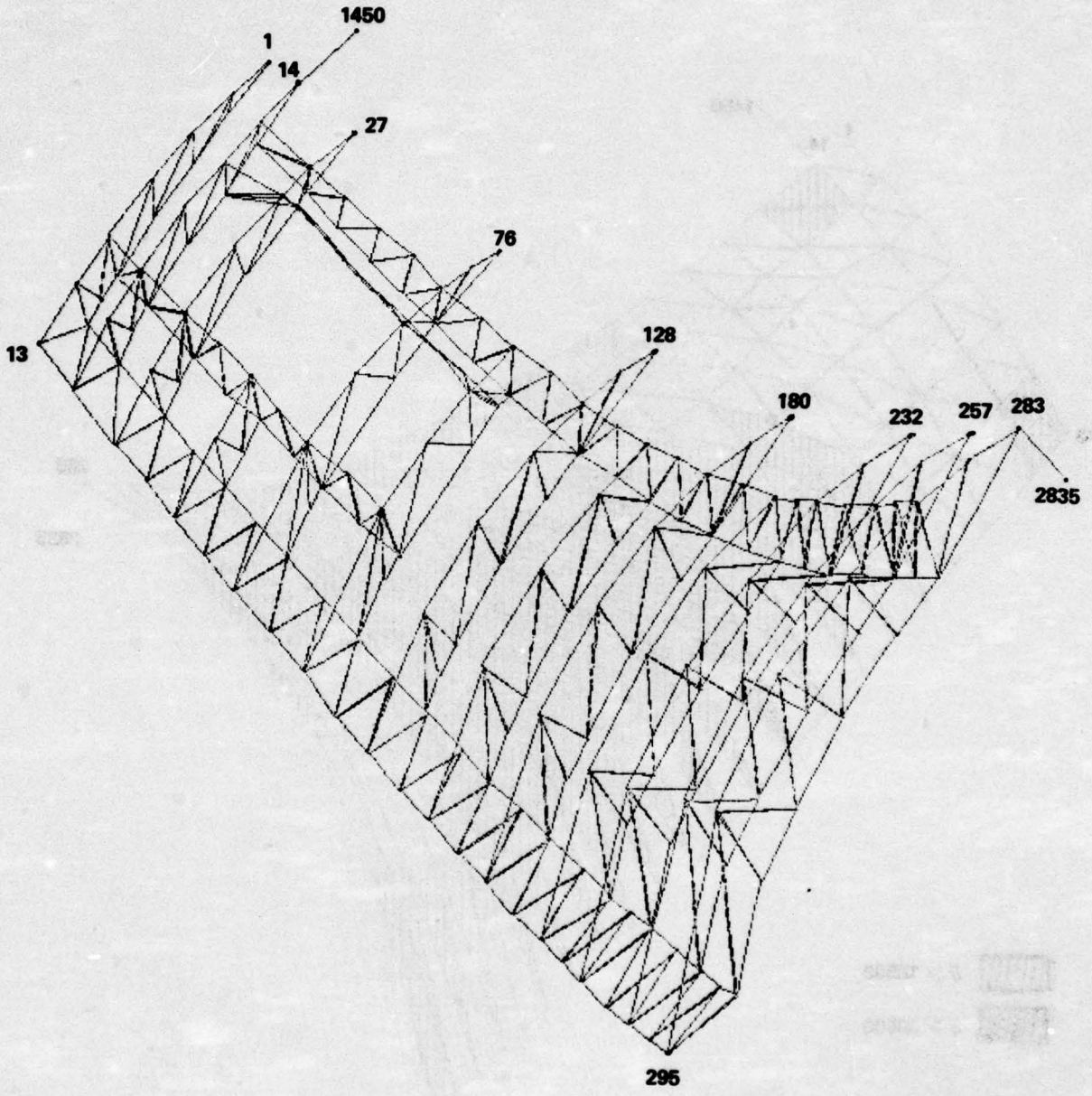

FIG. 9 DEFORMED SHAPE OF RIBS AND LONGERONS; 10 PSI STATIC LOAD

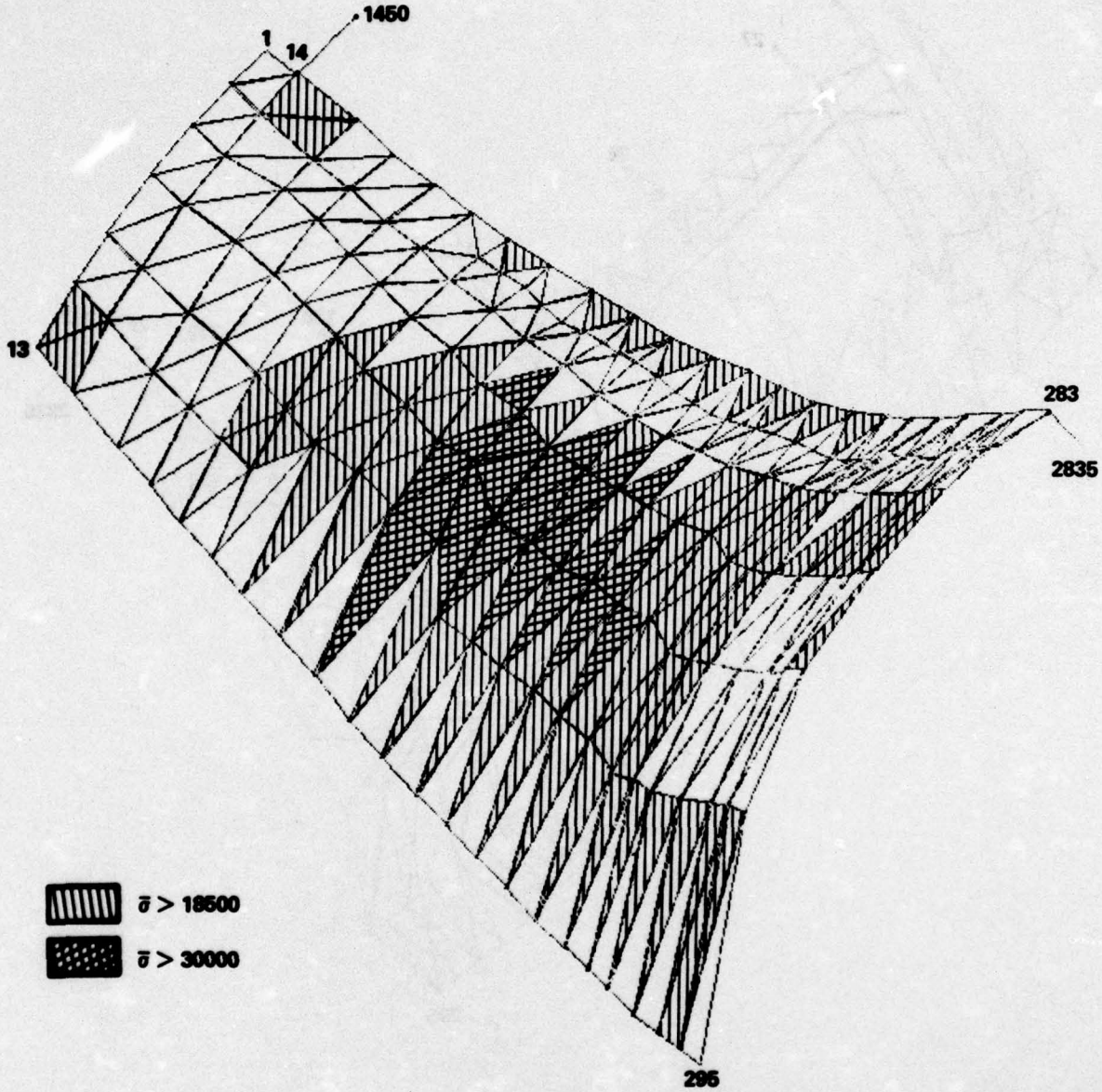

FIG. 10 STRESS DISTRIBUTION IN OUTER SKIN; 10 PSI STATIC LOAD

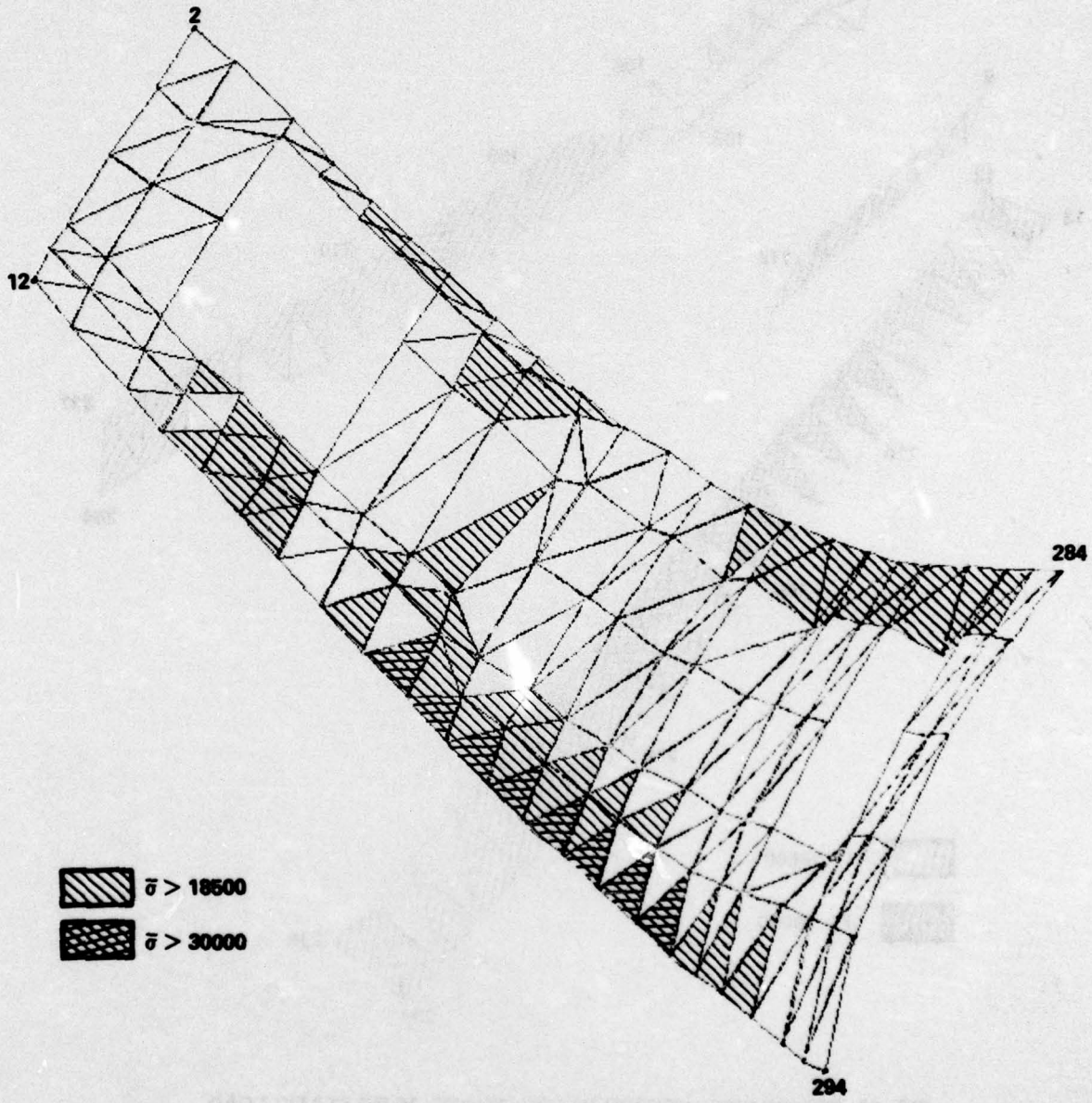

FIG. 11 STRESS DISTRIBUTION IN INNER SKIN; 10 PSI STATIC LOAD

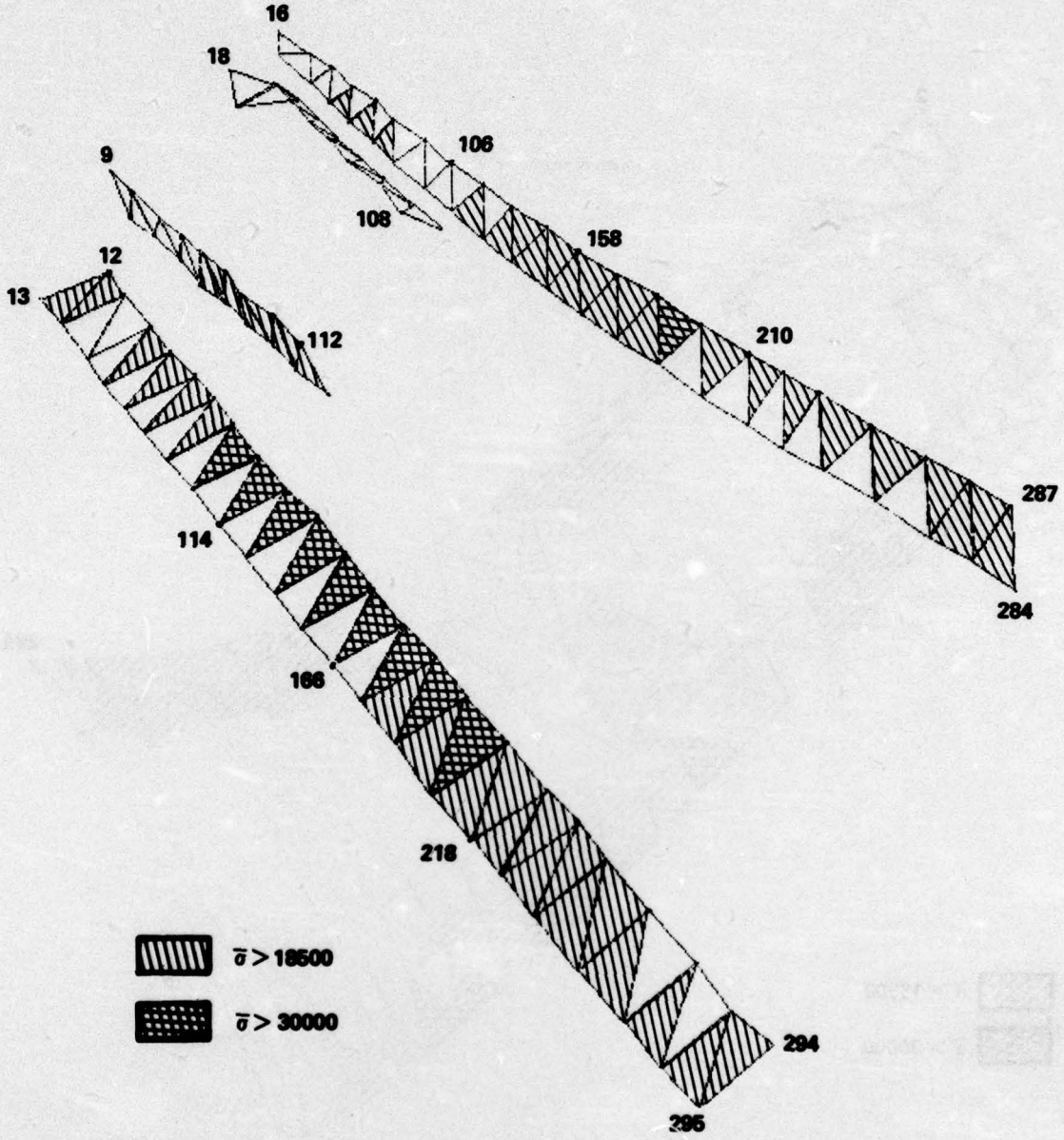

FIG. 12 STRESS DISTRIBUTION IN LONGERONS; 10 PSI STATIC LOAD

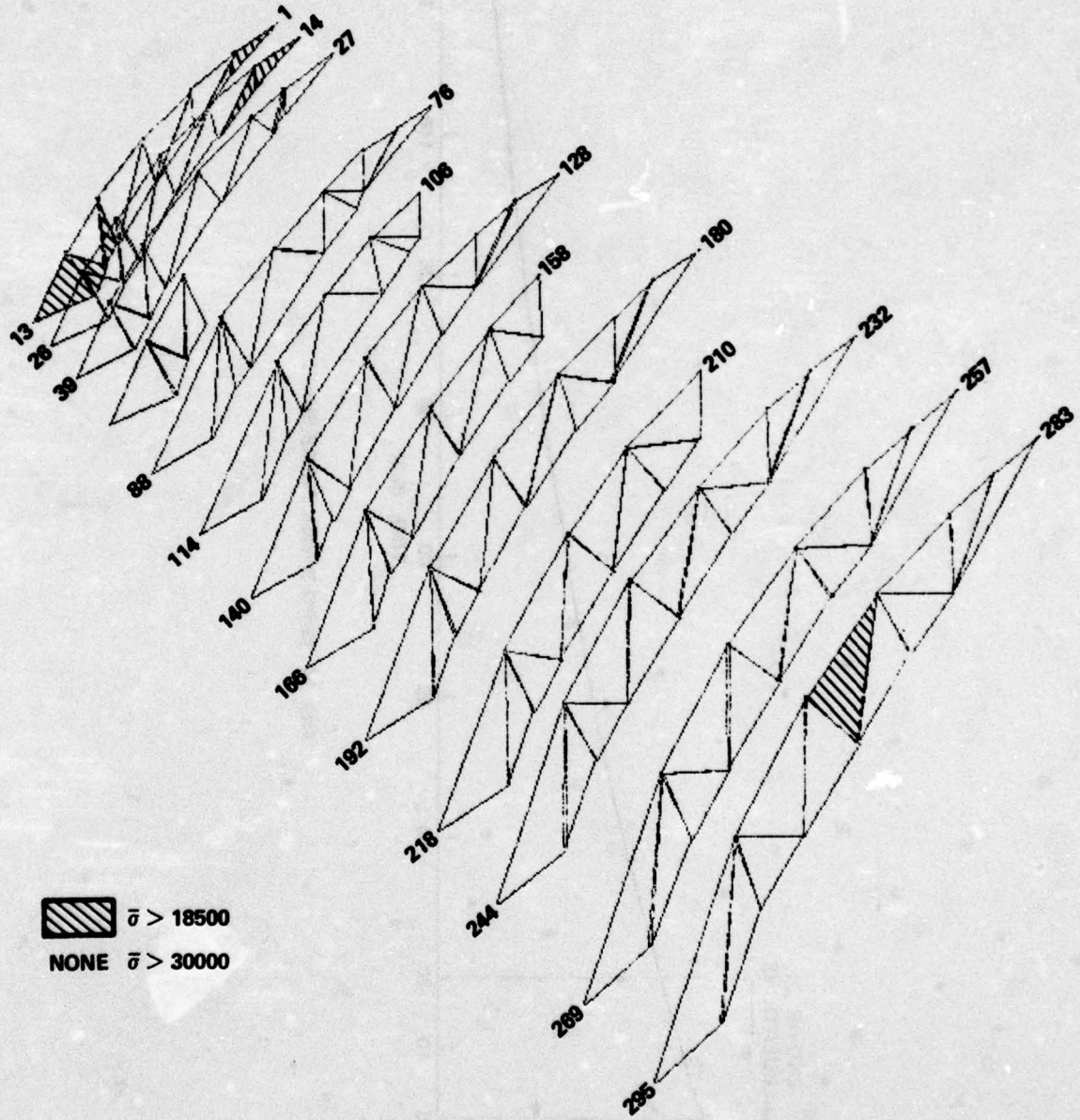

FIG. 13 STRESS DISTRIBUTION IN RIBS; 10 PSI STATIC LOAD

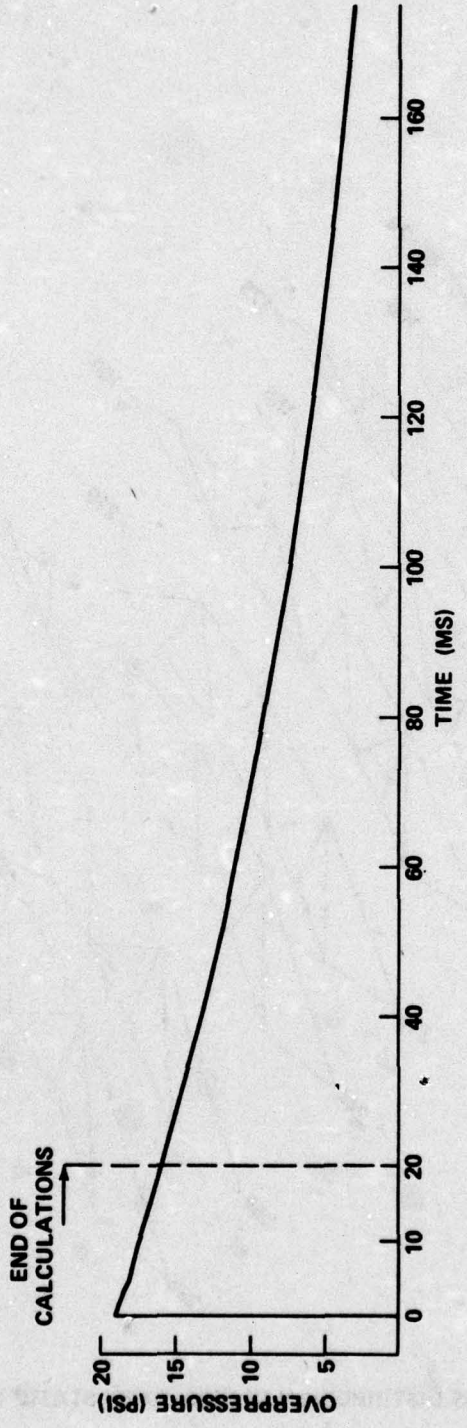

FIG. 14 19 PSI SHOCK PULSE SHAPE

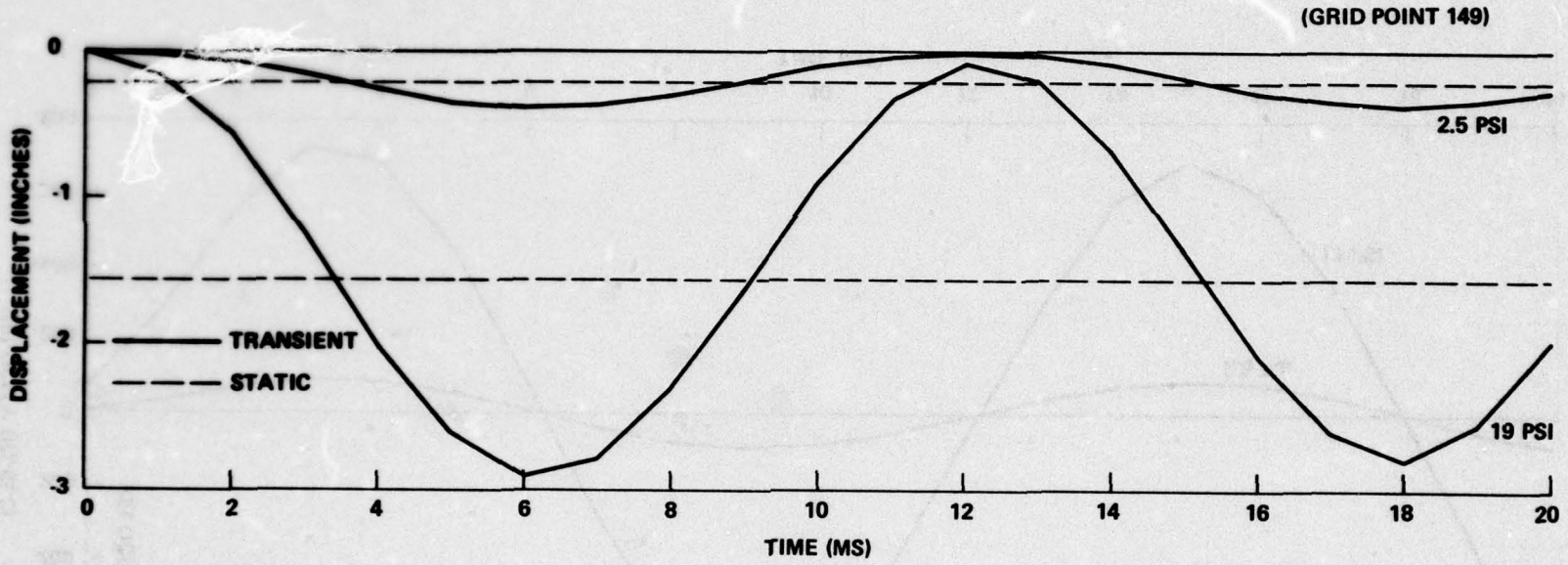

FIG. 15 NORMAL DISPLACEMENT NEAR CENTER OF DOOR; TRANSIENT LOADS

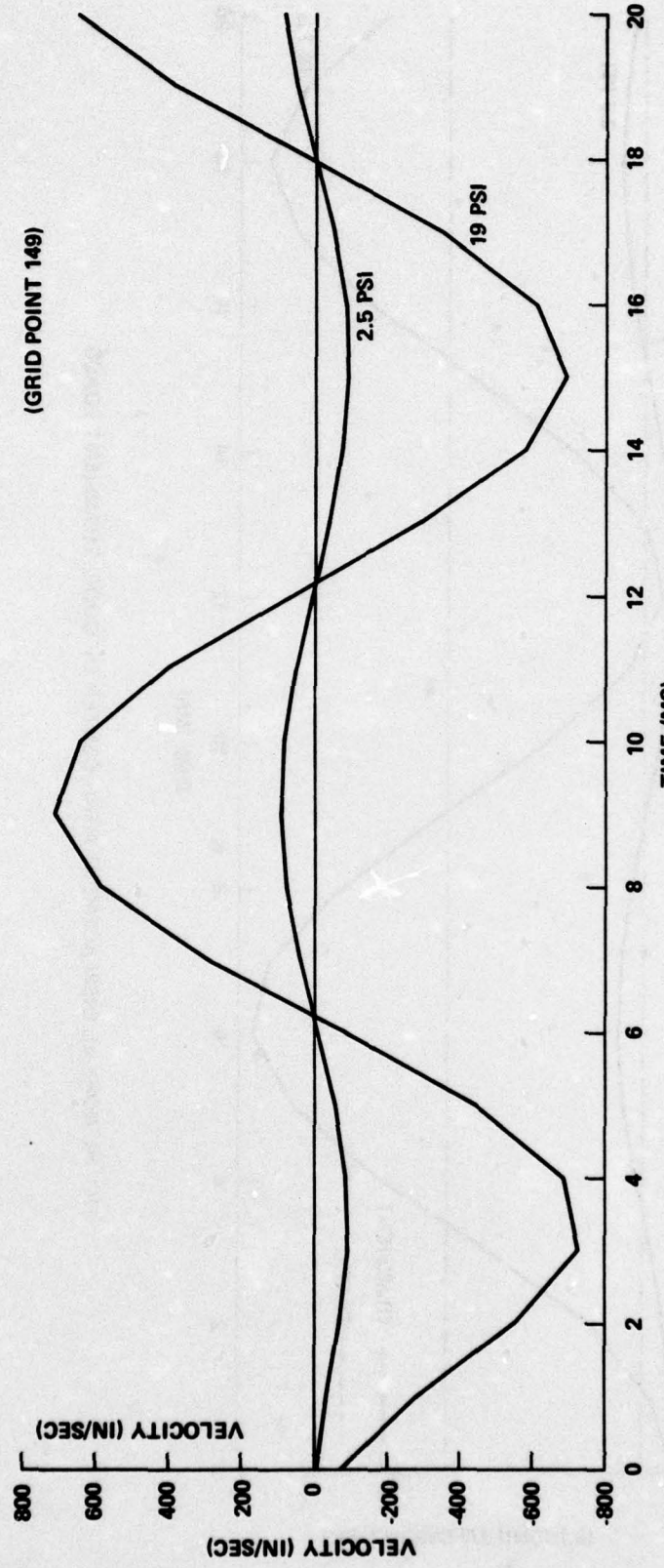

FIG. 16 NORMAL VELOCITY NEAR CENTER OF DOOR; TRANSIENT LOADS

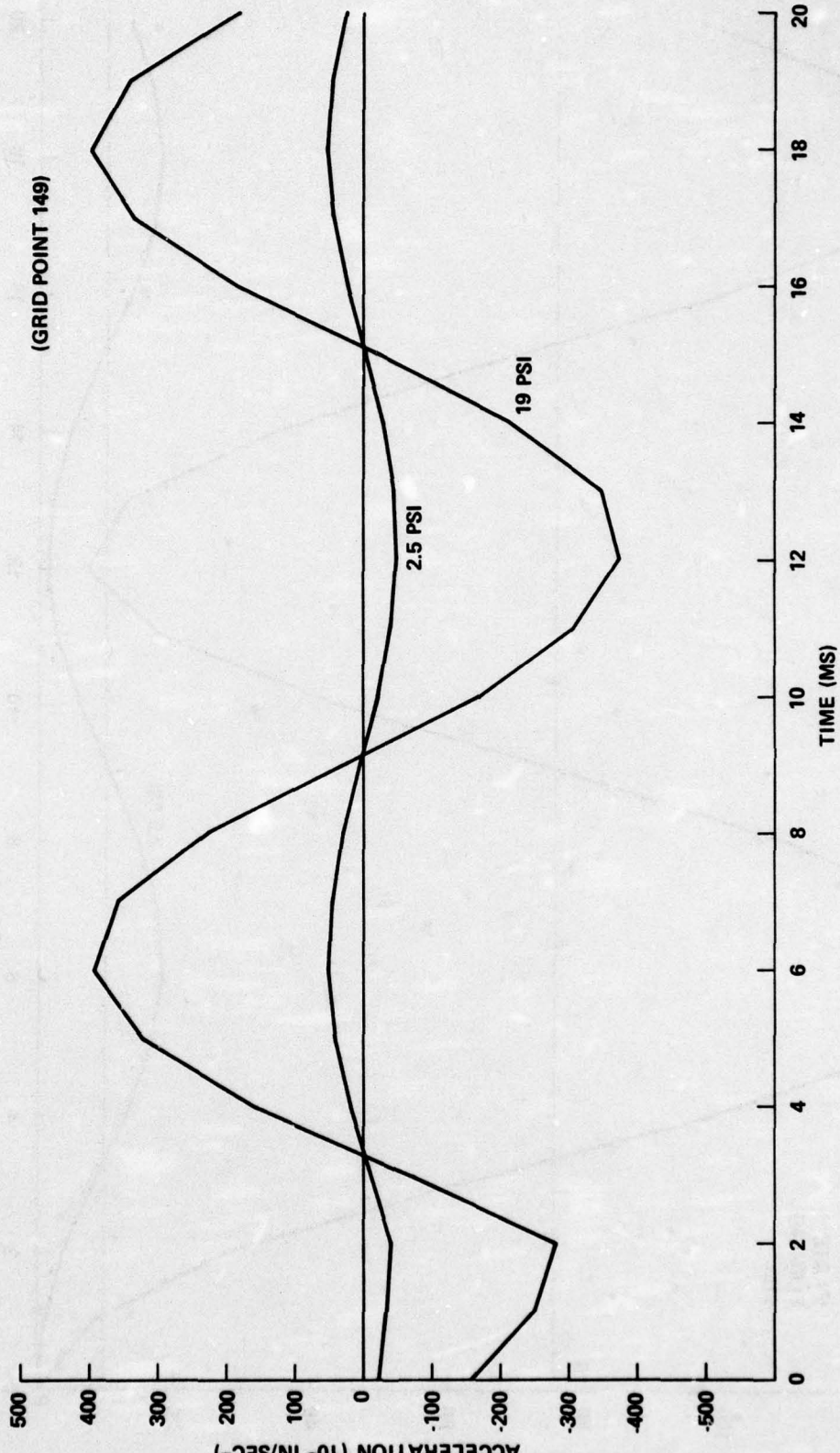

FIG. 17 NORMAL ACCELERATION NEAR CENTER OF DOOR; TRANSIENT LOADS

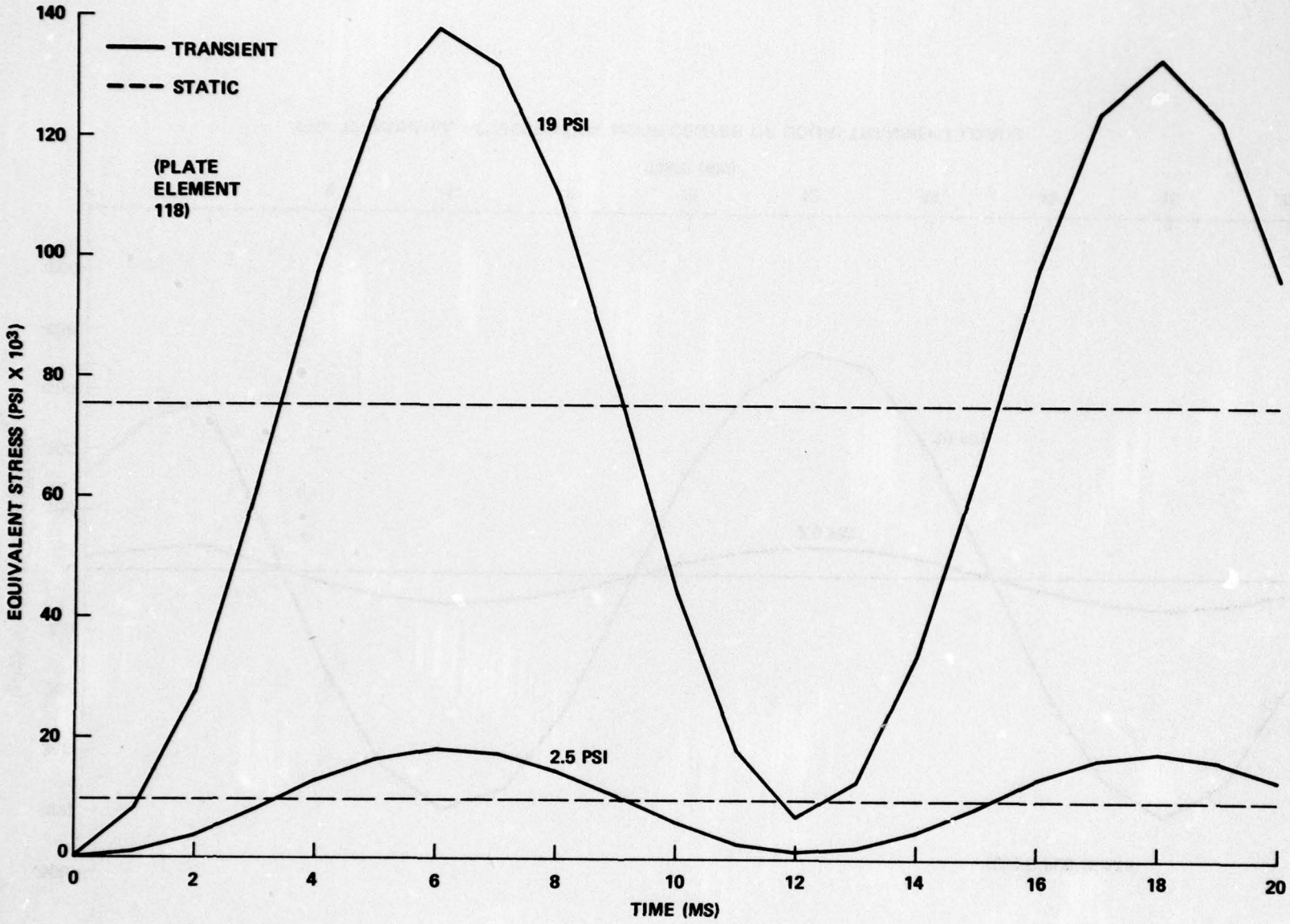

FIG. 18 EQUIVALENT STRESS IN MOST HIGHLY STRESSED ELEMENT; TRANSIENT LOADS

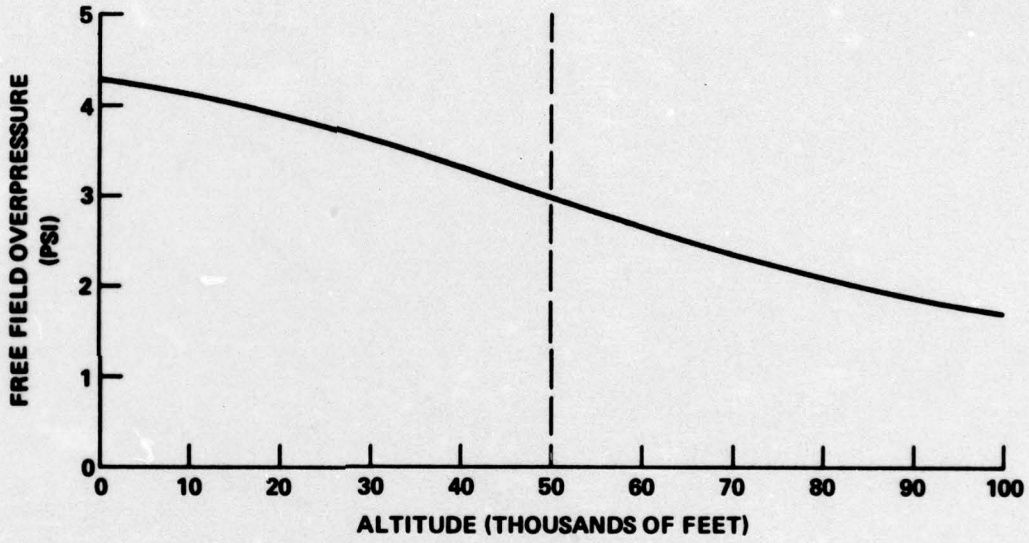

FIG. 19 FREE FIELD OVERPRESSURE REQUIRED AT VARIOUS ALTITUDES TO PRODUCE A REFLECTED PRESSURE OF 9.4 PSI

DISTRIBUTION

	Copies
Commander Naval Air Systems Command Washington, D. C. 20361 Attn: AIR-03C AIR-03PAF AIR-05 AIR-503 AIR-52023 AIR-5204 AIR-533 AIR-5313 AIR-5315 AIR-53233 AIR-350 AIR-350-T1 AIR-360 AIR-510 AIR-510A3 AIR-520 PMA-234 PMA-235 PMA-240 PMA-244	2
Commander Naval Sea Systems Command Washington, D. C. 20360 Attn: SEA-03A SEA-031 SEA-033 SEA-0352 SEA-6515	
Chief of Naval Operations Washington, D. C. 20350 Attn: NOP-604C3 NOP-604D2 NOP-098C NOP-620F NOP-620E NOP-985 NOP-985F2 NOP-506 NOP-622C NOP-096 NOP-96C NOP-951	

DISTRIBUTION (cont.)

Copies

Chief of Naval Research
800 N. Quincy Street
Arlington, VA 22217
Attn: Code 460

Commander
Naval Electronic Systems Command
Headquarters
Washington, D. C. 20360
Attn: ELEX 0512
ELEX 033

Chief of Naval Material
Navy Department
Washington, D. C. 20360 2
Attn: MAT 0323, Mr Jaffe

Assistant Secretary of the Navy
Research and Development
Washinton, D. C. 20350
Attn: Mr. H. Sonnemann

Commander
Naval Air Development Center
Johnsville, Warminister, PA 18974
Attn: Dr. G. T. Chisum
A. M. Stoll

Commanding Officer
Naval Weapons Evaluation Facility
Kirtland, AFB, NM 87117 2
Attn: Mr. Larry Oliver

Commander
Naval Weapons Center
China Lake, CA 93555

Commander
Naval Electronic Laboratory Center
San Diego, CA 92152
Attn: M. Lichtman

Commander
Naval Communications Command
4401 Massachusetts Avenue, N.W.
Washington, D. C. 20390
Attn: N-2

DISTRIBUTION (cont.)

Copies

Commander
Naval Ship Engineering Center
Prince Georges Center
Hyattsville, MD 20782
Attn: Y. Park, Code 6105C

Commander-in-Chief
U. S. Atlantic Fleet
Norfolk, VA 23511
Attn: Document Control

Commander-in-Chief
U. S. Pacific Fleet
EPO San Francisco, CA 96610
Attn: Document Control

Commander
Operational Test and Evaluation Force
Naval Base
Norfolk, VA 23511

Director
Defense Nuclear Agency
Washington, D. C. 20305
Attn: Dr. E. C. La Vier
Mr. J. Kelso
MAJ S. Kennedy
MAJ W. Adams
CDR D. M. Alderson
LCOL M. I. Kovel

Director
Armed Forces Radiobiology Research Institute
Defense Nuclear Agency
Bethesda, MD 20014
Attn: CAPT M. I. Varon
LCOL J. Cable

Commander
Aerospace Medical Research Laboratory
Air Force Systems Command
Wright Patterson Air Force Base, OH 45433
Attn: Mr. G. P. Chubb

Director
Strategic Systems Project Office
Crystal Mall Number 3
Washington, D. C. 20390
Attn: SP-27331

DISTRIBUTION(cont.)

Copies

Director of Defense Research and Engineering
Office of the Secretary of Defense
Washington, D. C. 20301

Chief of Research and Development
Department of the Army
Washington, D. C. 20310
Attn: Atomic Division

Defense Documentation Center 12
Cameron Station
Alexandria, VA 22314

Commanding Officer
Army Combat Development Command
Nuclear Agency
Fort Bliss, TX 79916

Commanding Officer
Eustis Directorate
Army Air Mobility Research
and Development Laboratory
Fort Eustis, VA 23604
Attn: S. Pociluyko

Deputy Chief of Staff, Research and Development
Department of the Air Force
Washington, D. C. 20330
Attn: RDQPN